Compact Stars

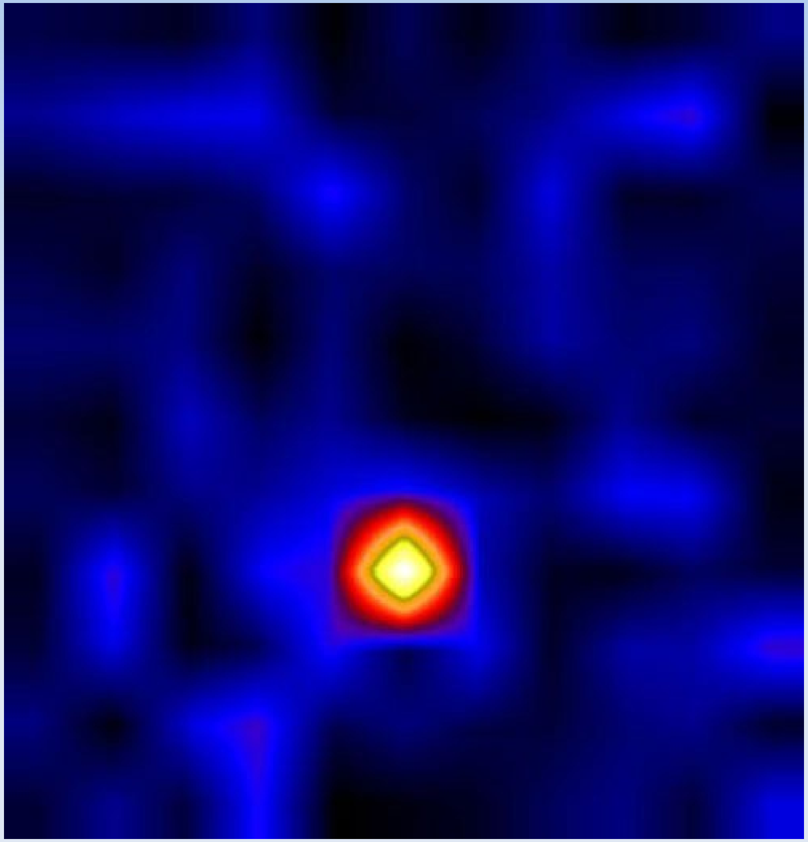

Lecture 9

Summary of previous lecture

- I talked about the gamma ray bursts as the extragalactic jet sources. In contrary to QSOs, GRBs are transient.
- I described their osberved properties (spectra, lightcurves), their phenomenology (bimodal duration distribution), and constraints for models of the GRB origin.
- I mentioned historical models of GRBs, selected satellite missions which observed them, and modern ideas about the short and long bursts progenitors.
- The historical debate on the distance scale to GRBs was won by B. Paczyński who provided arguments on their cosmological nature.
- The first ever article on arXiV (April 1st 1992) was devoted to Gamma Ray Bursts. It proved the power of internet in dissemination of scientific results.

Summary of the previous lecture

- I showed some results of GR MHD simulations of jet launching from GRB engines
- By solving continuity and stress-energy conservation equations, with magnetic field evolution described by Maxwell equations, we can follow the evolution of magnetized outflow in gravitational field of black hole.
- Fixed Kerr metric is used in these calculations, with proper coordinate transformations to allow the plasma accrete under the horizon.
- The energy flux integrated over the BH horizon, can be extracted through the Blandford-Znajek process and provide power to accelerate remote jets.

Today

- Long and short GRB engines
- Models with proper microphysics of dense and hot matter in the central engine
- Neutrino cooling

Long GRBs: observations

- Red bump in lightcurves and lines in spectra: in the long GRBs SN signatures
- Variable profiles
- Statistics (star formation rate); host galaxies etc.

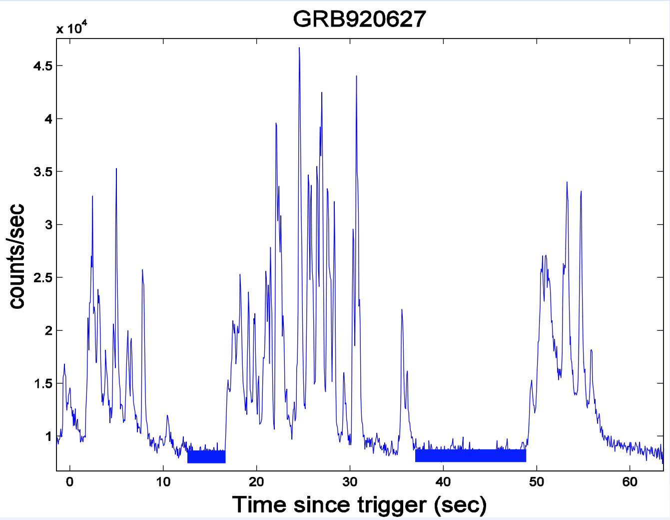

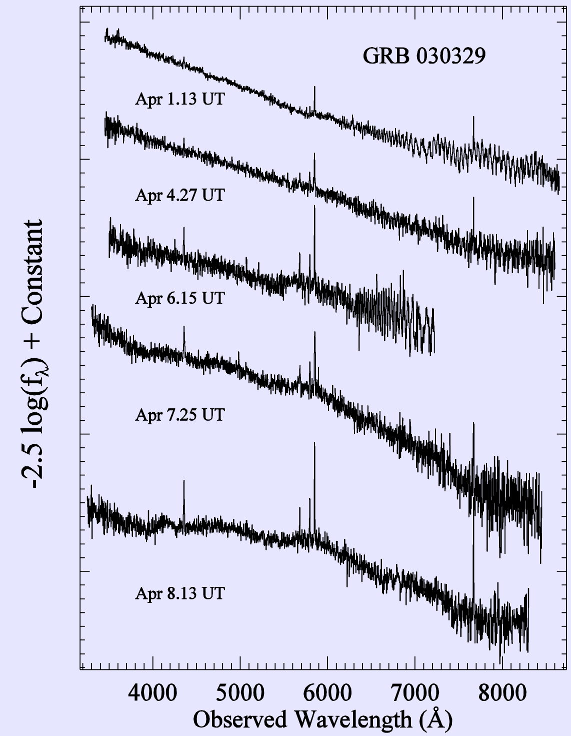

Stanek et al. (2003)

Short GRBs: observations

- Lack of SN-associacion
- Localized in old stellar populations in elliptical galaxies
- Explosions with 'baryon clean' high Lorentz factor ejecta result in X-ray aferglow
- Off-set from the host centers: prediction of the NS-NS merger model is the 'natal kicks'
- Prospects for GW detections, and r-process nucleosynthesis (see review by E. Berger, 2014, A&A Rev). Confirmed in 2017.

Cosmological effects

- Redshifts obtained mostly for long, and for a sub-sample of short GRBs (selection).
- V/Vmax distribution suggested populationss evolve in non-Euclidean space (cosmological), but differently placed than long GRBs (T. Piran).
- Alternative explanation is that GRB populations evolve in time.

Schematic engine of a GRB

- Engine composed of rotating black hole and accretion disk is common for different progenitor scenarios
- Matter in the accretion disk is supplied ba fallback of the collapsin star envelope or from the tidally disrupted neutron stars

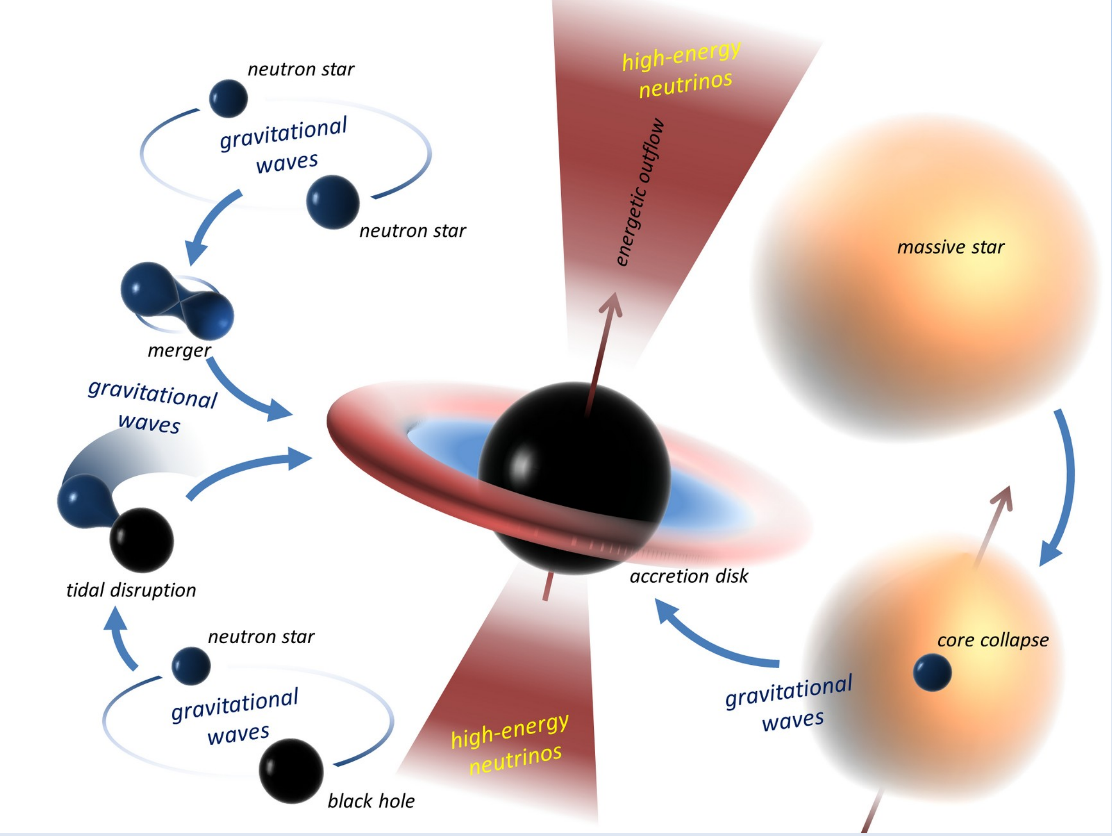

Conditions in the disk

- Temperature > 1 MeV: electron-positron pairs must be produced
- Nuclear densities: electrons partially degenerate
- Neutronisation processes: equilibrium p/n established

Weak interactions:

$p + e^{-} \rightarrow n + \nu_e$

$n + e^{+} \rightarrow p + \nu^{-}_{e}$

Equation of state

- The total pressure must include the contributions from gas, radiation, and degenerate electrons:

$$P = P_{gas} + P_{rad} + P_{deg} = \frac{k}{m_p} \rho T \left(\frac{1}{4} + \frac{3}{4} X_{nuc} \right) + \frac{11}{12} a T^4 + 2\pi h \frac{c}{3} \left(\frac{3}{8} \pi m_p \right)^{4/3} \left(\frac{\rho}{\mu_e} \right)^{4/3}$$

where mass fraction of free nucleons depends non-linearly on density and temperature (Popham et al. 1999; Di Matteo et al. 2002; Janiuk et al. 2004)

- In more advanced modeling, the equation of state must be computed numerically by solving the balance of nuclear reactions (Yuan 2005; Janiuk et al. 2007; cf. also Lattimer & Swesty 1991; Setiawan et al. 2004)

EOS of degenerate electrons

- Electron degeneracy is quantum mechanical effect. Electrons in the gas are confined in the volume and must obey Pauli exclusion principle – they cannot occupy the same state.
- Each particle in the Fermi gas has kinetic energy of $E=p^2/2m$. Every possible momentum up to the Fermi momentum can be occupied.
- When particles energies are at relativistic limit, E=pc, the pressure scales with density as

$$P_e = 1.23 \cdot 10^{15} \left(\frac{\rho}{\mu_e}\right)^{4/3} [cgs]$$

Limits on temperature-density plane

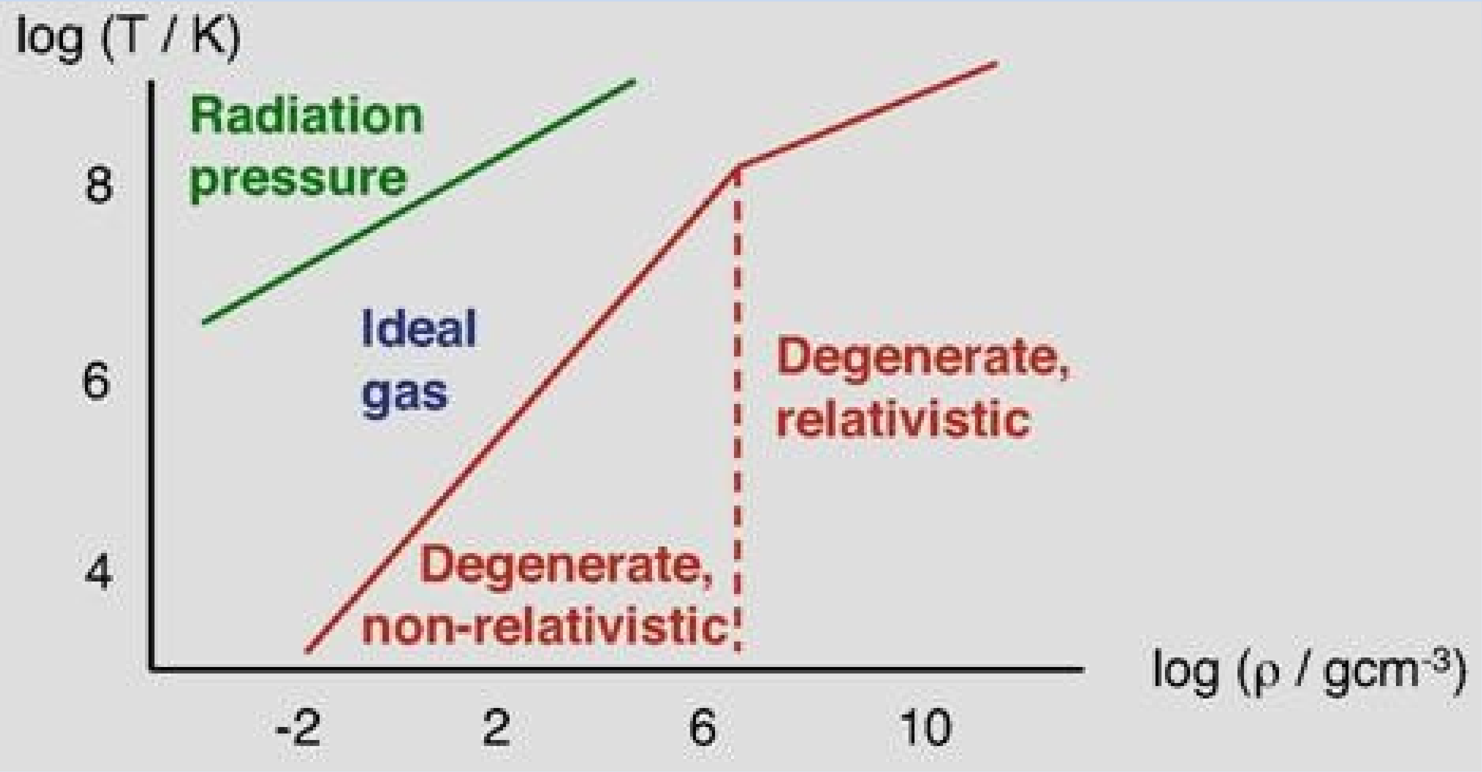

GRB Disk stationary solutions

- First results with α-disk prescription were obtained by 1999 (Popham et al.)
- Helium nuclei are formed at such densities and temperatures (NSE)
- Stationary models turned into time-dependent 1_d hydrodynamics (Janiuk et al. 2004)

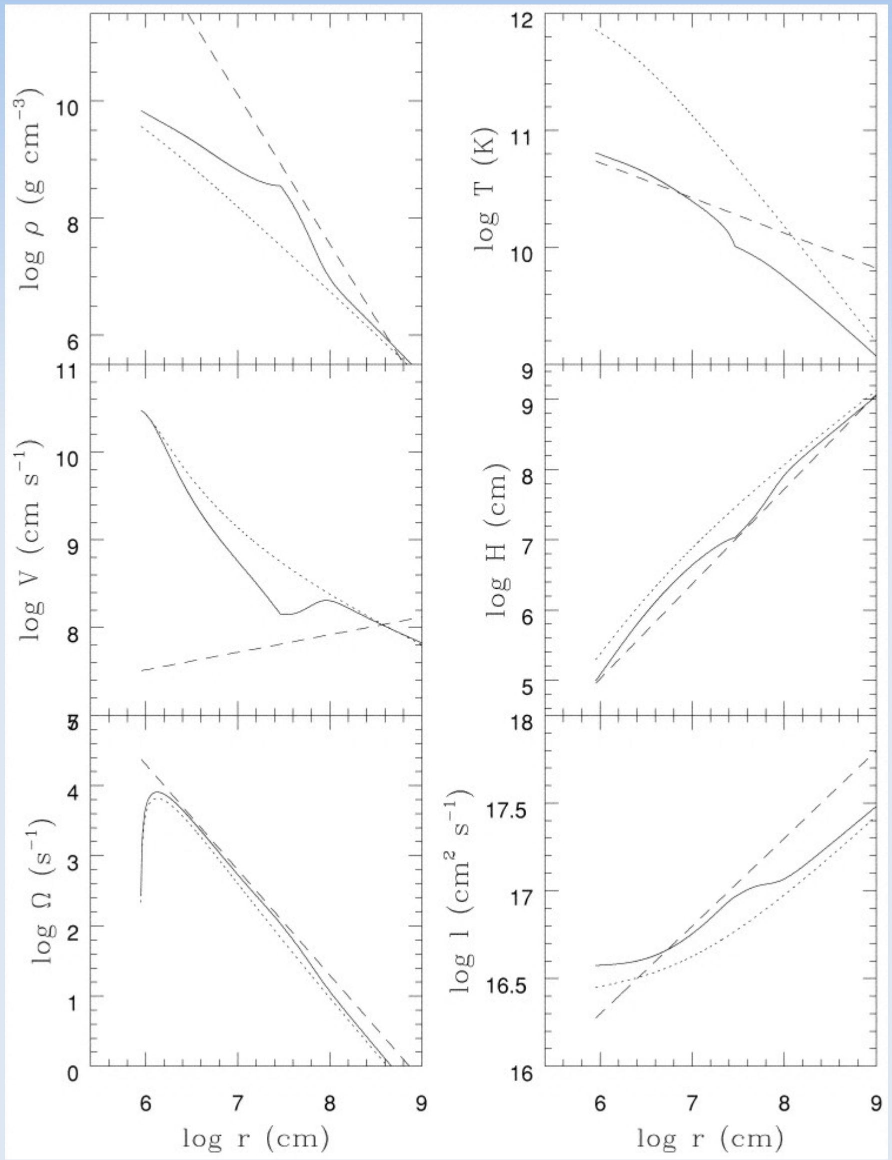

Popham, Woosley, & Fryer, 1999, ApJ, 518, 1

Conditions in the NDAF disk

- Disks may be opaque to neutrinos → two-stream approximation introduced by Di Matteo et al. (2002)
- Helium may be photodissociated.
- Photons: totally trapped
- Advective cooling
- Neutrinos: absorbed and scattered, if the opacities are high. Two stream approximation.

$$L_\nu = \int Q_\nu dV = \int 7/8\,\sigma T^4 \sum_{i=e,\mu} \frac{1}{0.5(\tau_a + \tau_s) + \frac{1}{\sqrt{3}} + \frac{1}{3\tau_a}} dV$$

Neutrino luminosity

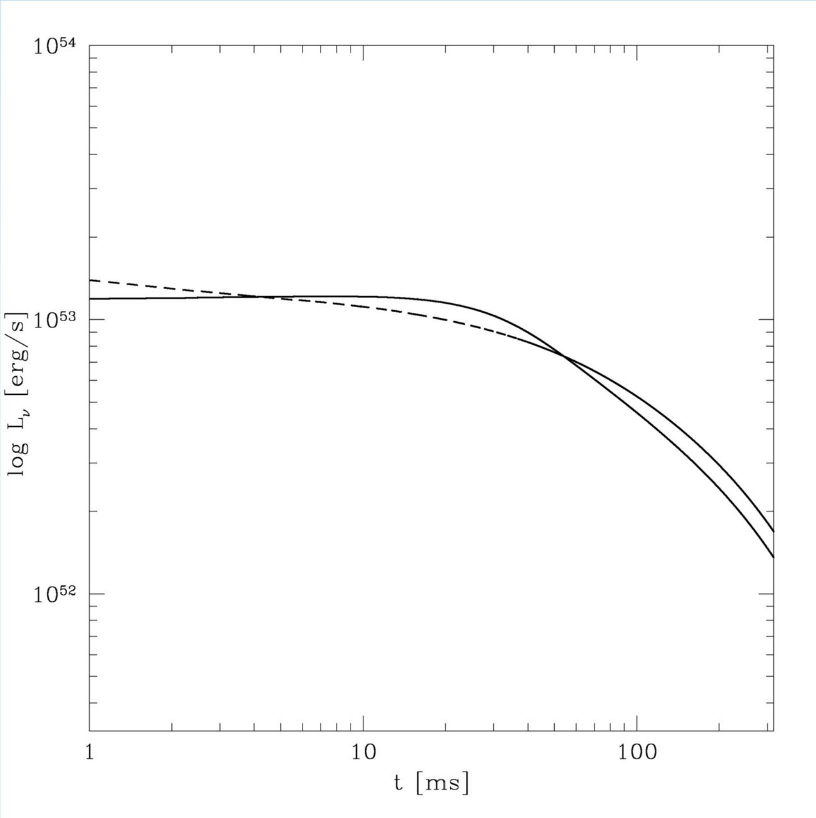

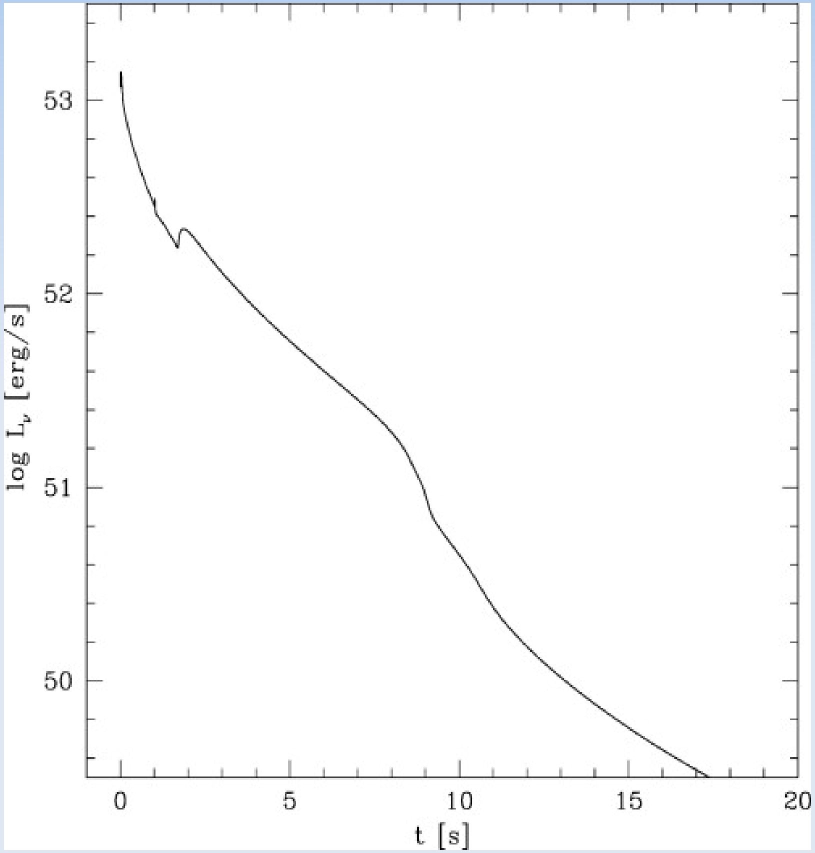

- Evolution of the neutrino luminosity for long and short GRB central engine

Janiuk A, Perna R., Di Matteo, T. Czerny B., 2004, MNRAS

Conditions in the central engine

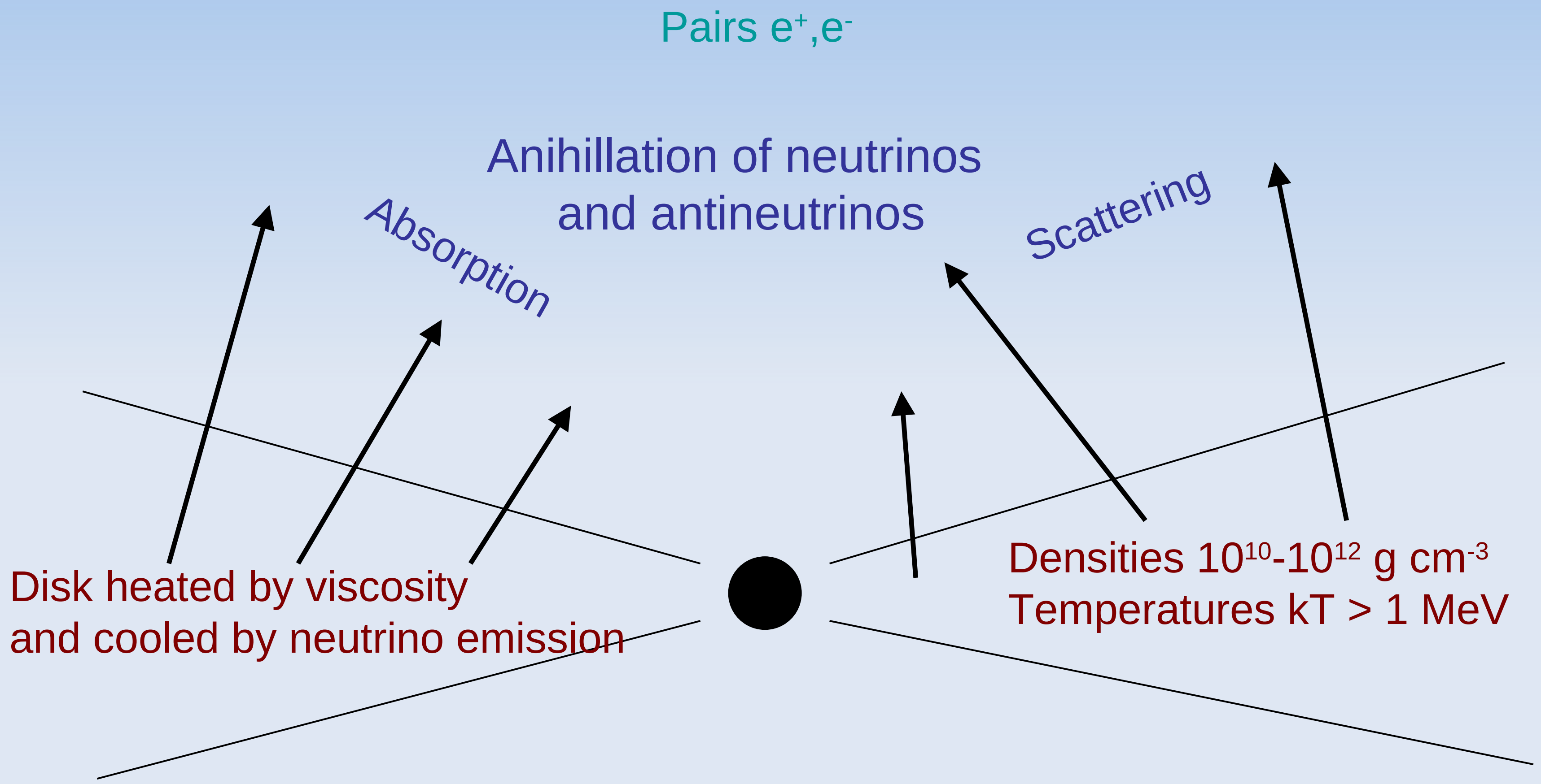

Neutrino annihilation

TABLE 3

NEUTRINO ANNIHILATION EFFICIENCY

$\dot{M}$ ($M_\odot$ s^{-1})	α	a	M ($M_\odot$)	L_ν (10^{51} ergs s^{-1})	$L_{\nu\bar{\nu}}$ (10^{51} ergs s^{-1})	Efficiency (%)
0.01	0.1	0	3	0.015	3.9×10^{-8}	0.0003
0.01	0.03	0	3	0.089	2.9×10^{-7}	0.0003
0.01	0.01	0	3	0.650	9.0×10^{-6}	0.001
0.01	0.1	0.5	3	0.036	5.9×10^{-7}	0.002
0.01	0.01	0	10	0.049	6.4×10^{-9}	10^{-5}
0.05	0.1	0.5	3	1.65	1.8×10^{-3}	0.11
0.1	0.1	0	3	3.35	3.0×10^{-3}	0.09
0.1	0.03	0	3	6.96	1.7×10^{-3}	0.02
0.1	0.01	0	3	6.15	8.0×10^{-4}	0.01
0.1	0.1	0.5	3	8.03	0.039	0.5
0.1	0.1	0.95	3	46.4	2.0	4.2
0.1	0.1	0.95	6	26.2	0.79	3.0
1.0	0.1	0	3	86.3	0.56	0.6
1.0	0.1	0.5	3	142	3.5	2.5
10.0[a]	0.1	0	3	(781)	(200)	(26)
10.0[a]	0.1	0.5	3	(1280)	(820)	(64)

[a] The assumption that the neutrinos are optically thin breaks down for accretion rates of 10 $M_\odot$ s^{-1} and above. The neutrino annihilation luminosities and energies listed for these high-accretion simulations are upper limits.

Hyperaccretion disk

- Model must account for coupling between degeneracy of matter and neutrino cooling. Cooling → lower temperature → degeneracy → low density of positrons → lower cooling → higher temperature

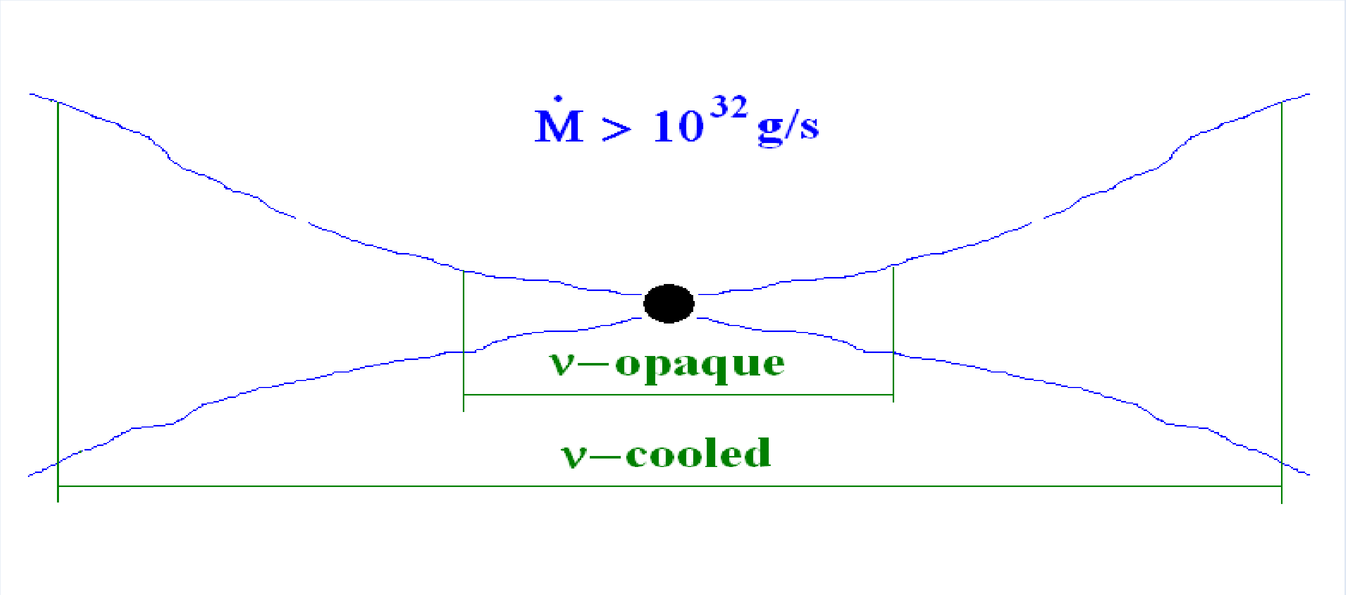

Chen & Beloborodov (2007)

Outskirts: gravitational instability

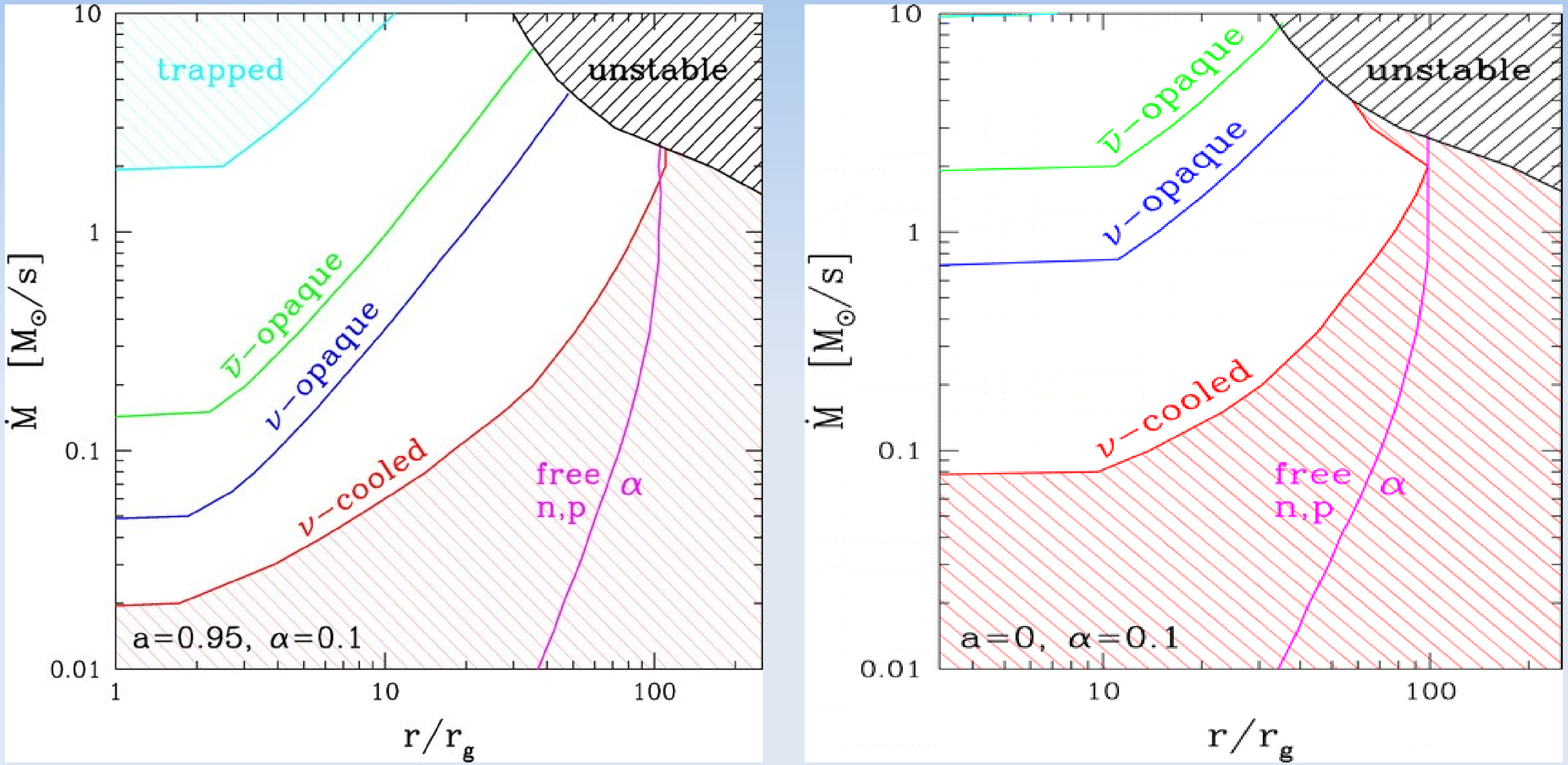

Chen & Beloborodov (2007)

Magnetar model

- Post-merger massive neutron star, with strong magnetic field ($B \sim 10^{15}$ G) and rapid rotation ($P \sim 1$ ms)
- Looses energy via magnetic dipole radiation
- Energy injection has characteristic spin-down timescale, defined by B and P

$$dE/dt \sim 10^{49} (B/10^{15}\ G)^2 (P/1ms)^{-4} \quad [erg/s]$$

(Zhang & Meszaros, 2001)

Magnetar model

- Magnetar model fits explain some of GRBs where a plateau phase is observed

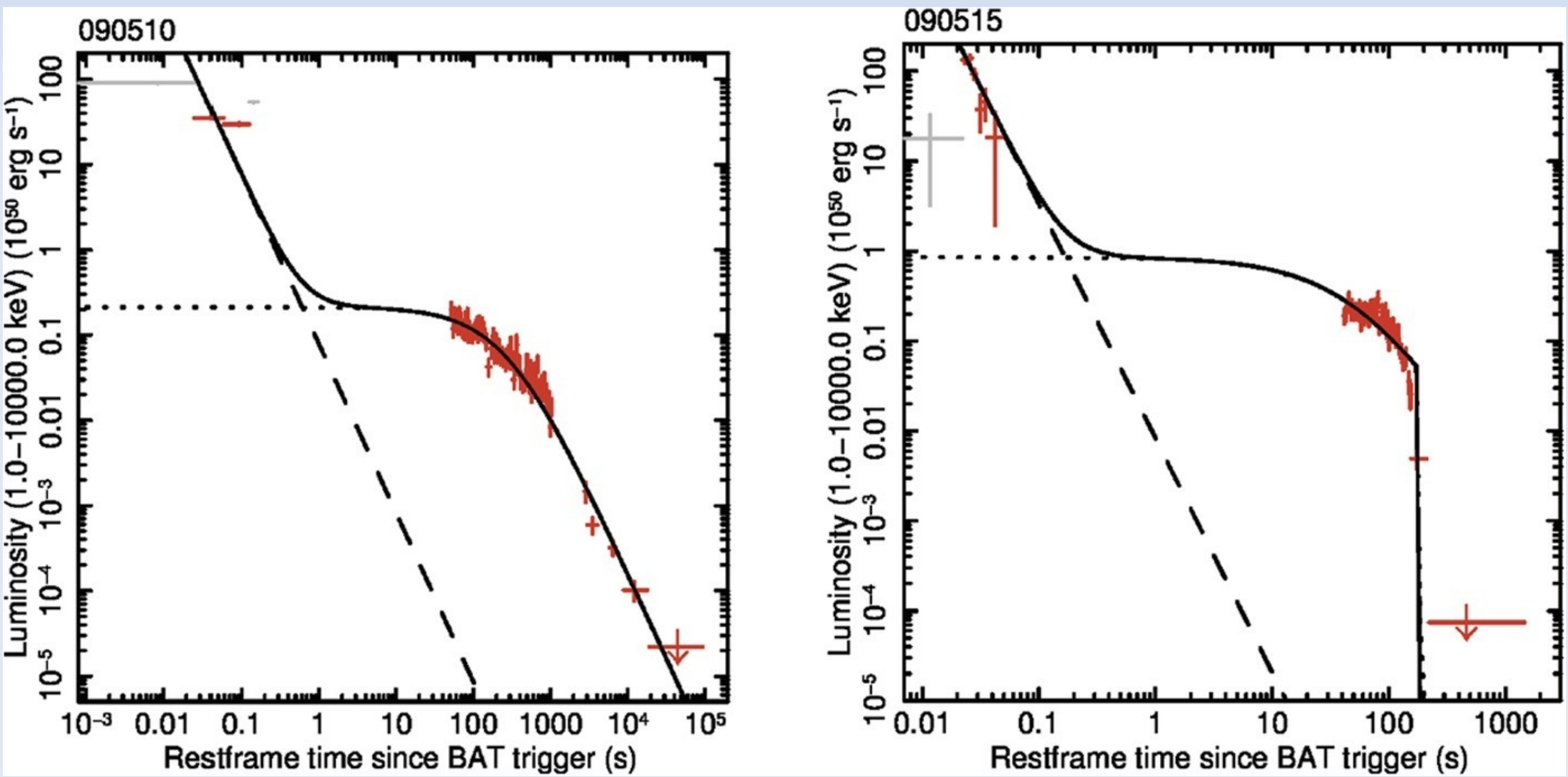

Swift BAT/XRT lightcurves (Rowlinson et al. 2013)

Magnetar model

- Another application of magnetar model is pre- and post-cursor in the prompt GRB

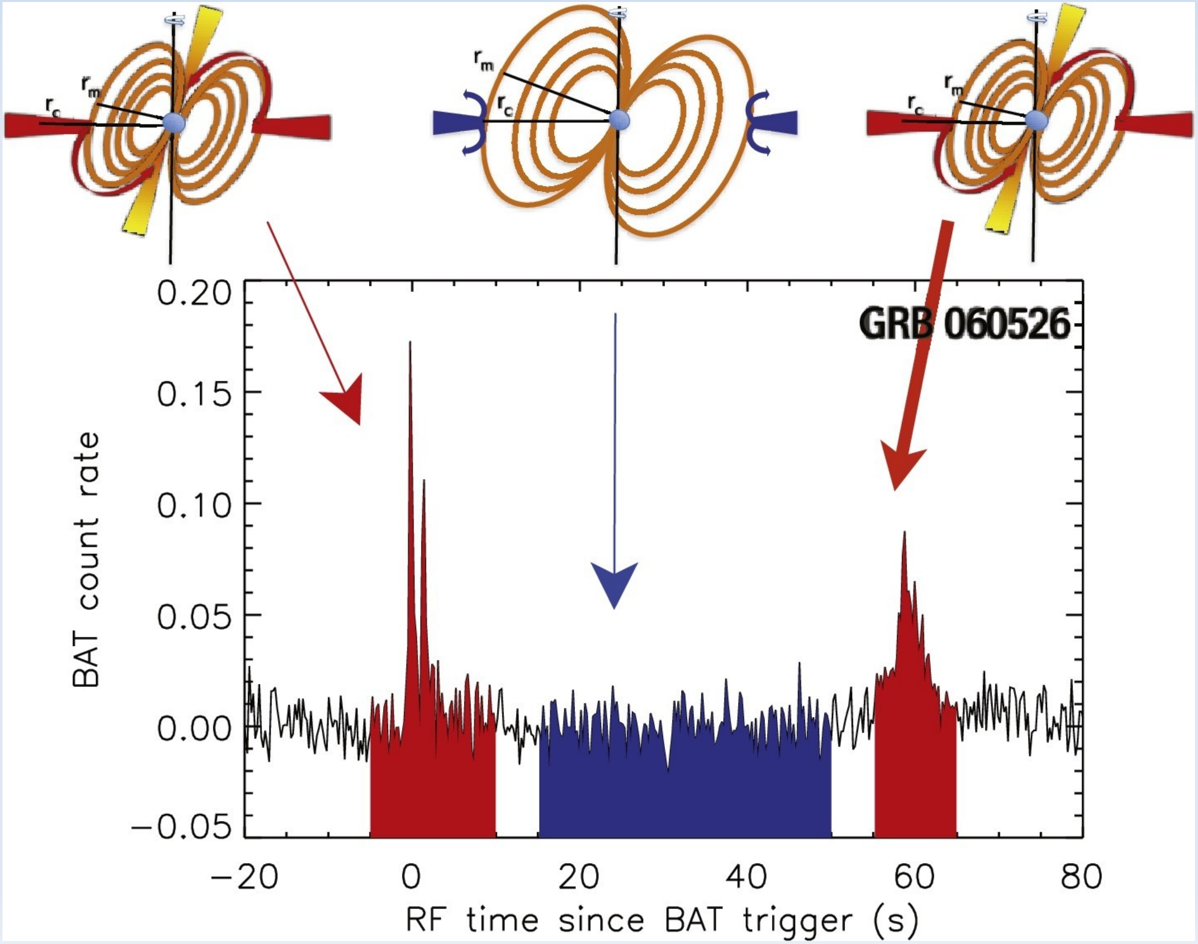

Swift/BAT count rate light curve of GRB 060526, with the main event and the post-cursor (red areas), and the quiescent time (blue areas).

Propeller and accretor phases may occur several times.

(Bernardini 2015).

Break

Degenerate gas in Hyperaccretion disk

- Hyperaccretion: rates of 0.01-10 M_{Sun}/s
- Chemical and pressure balance required by nuclear reaction rates
- These are given under arbitrary degeneracy of species
- Charge neutrality condition

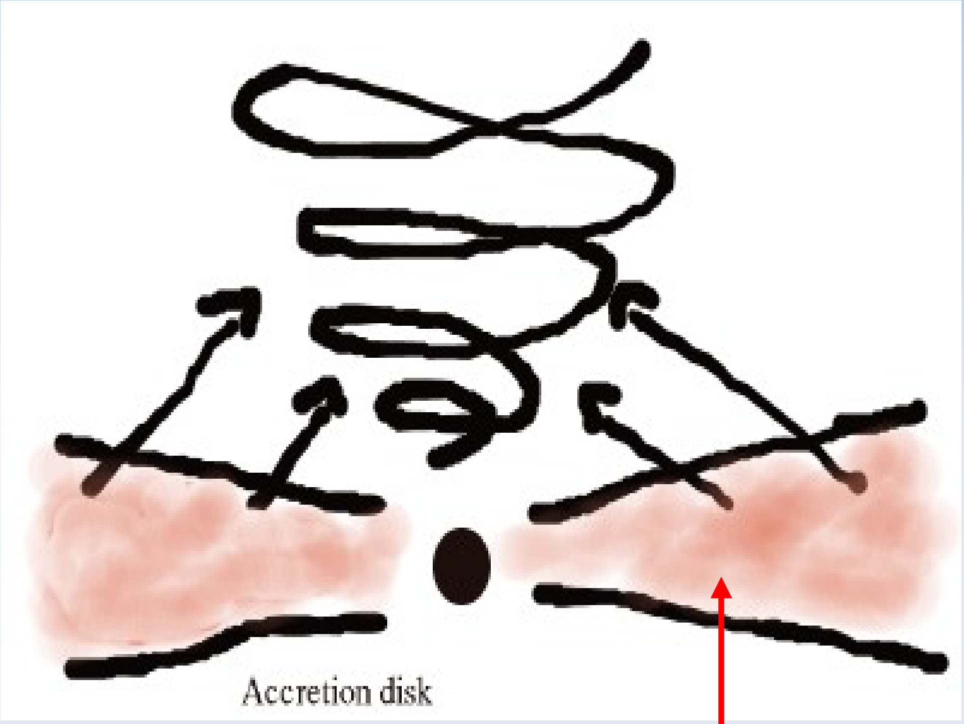

p, n, e^+, e^-
He,
ν_μ, ν_e, ν_τ
γ

Neutrino cooling

- The photons are totally trapped in the very opaque disk. The main cooling mechanism is the emission of neutrinos, via the following reactions:
  - Electron and positron capture on nucleons (URCA reactions) → electron neutrinos
  - Electron-positron pair anihillation (electron, muon and tau neutrinos)
  - Bremsstrahlung (all neutrino flavours)
- Emissivities in first two cases computed numerically (Itoh et al. 1996; Yakovlev 2005)

Numerical scheme for CE structure

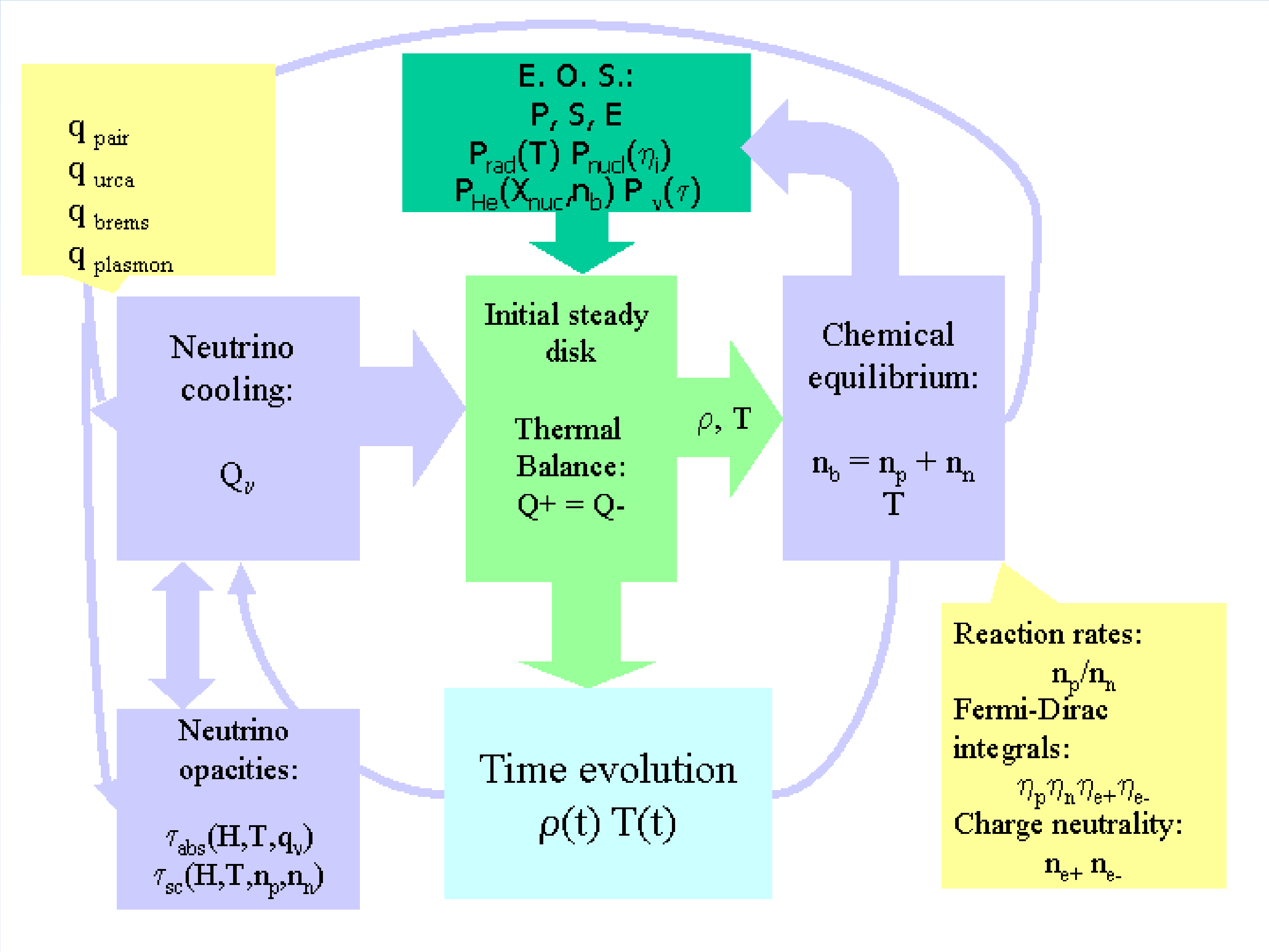

Janiuk, Yuan, Perna & Di Matteo (2007)

Density and temperature profiles

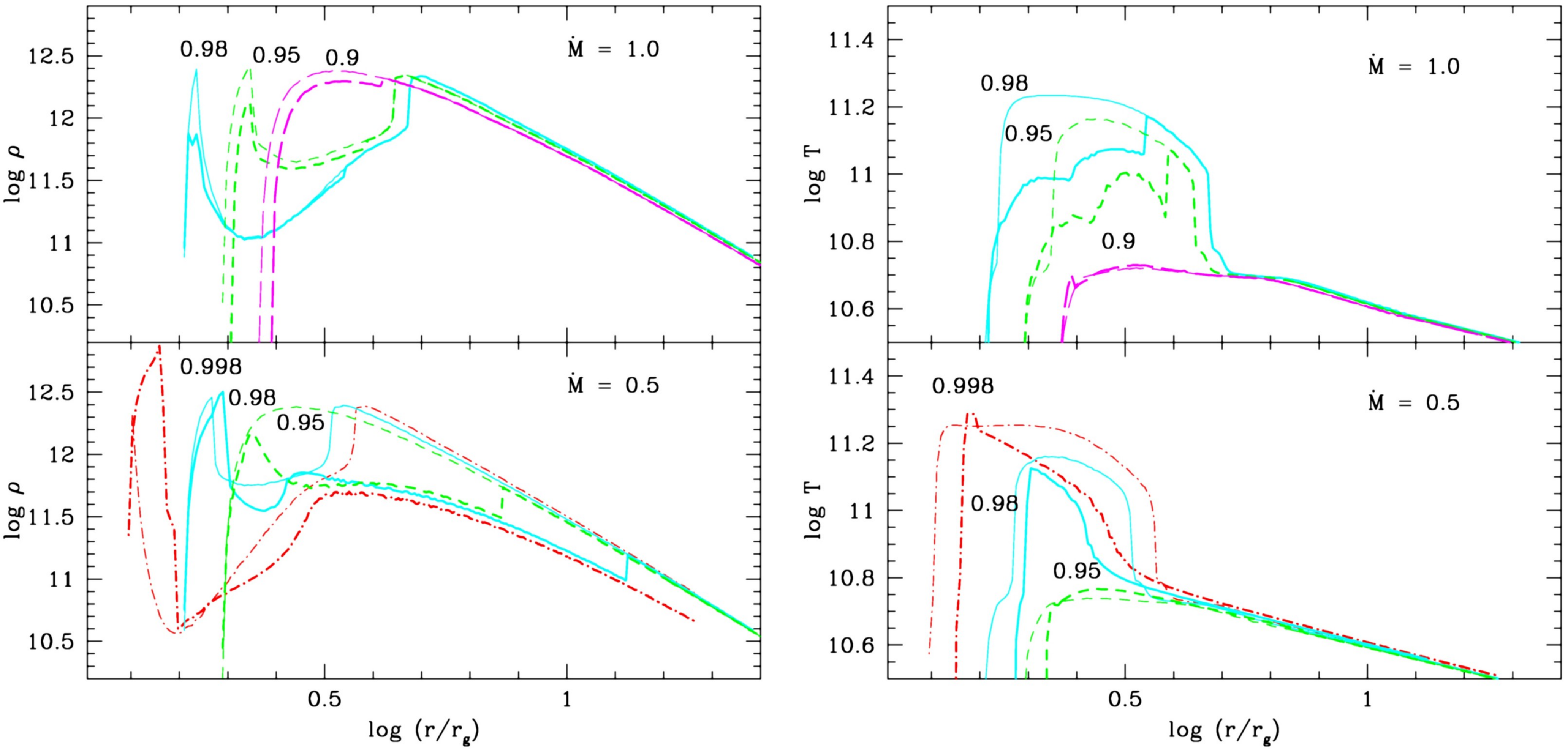

Inner disk: possibly unstable?

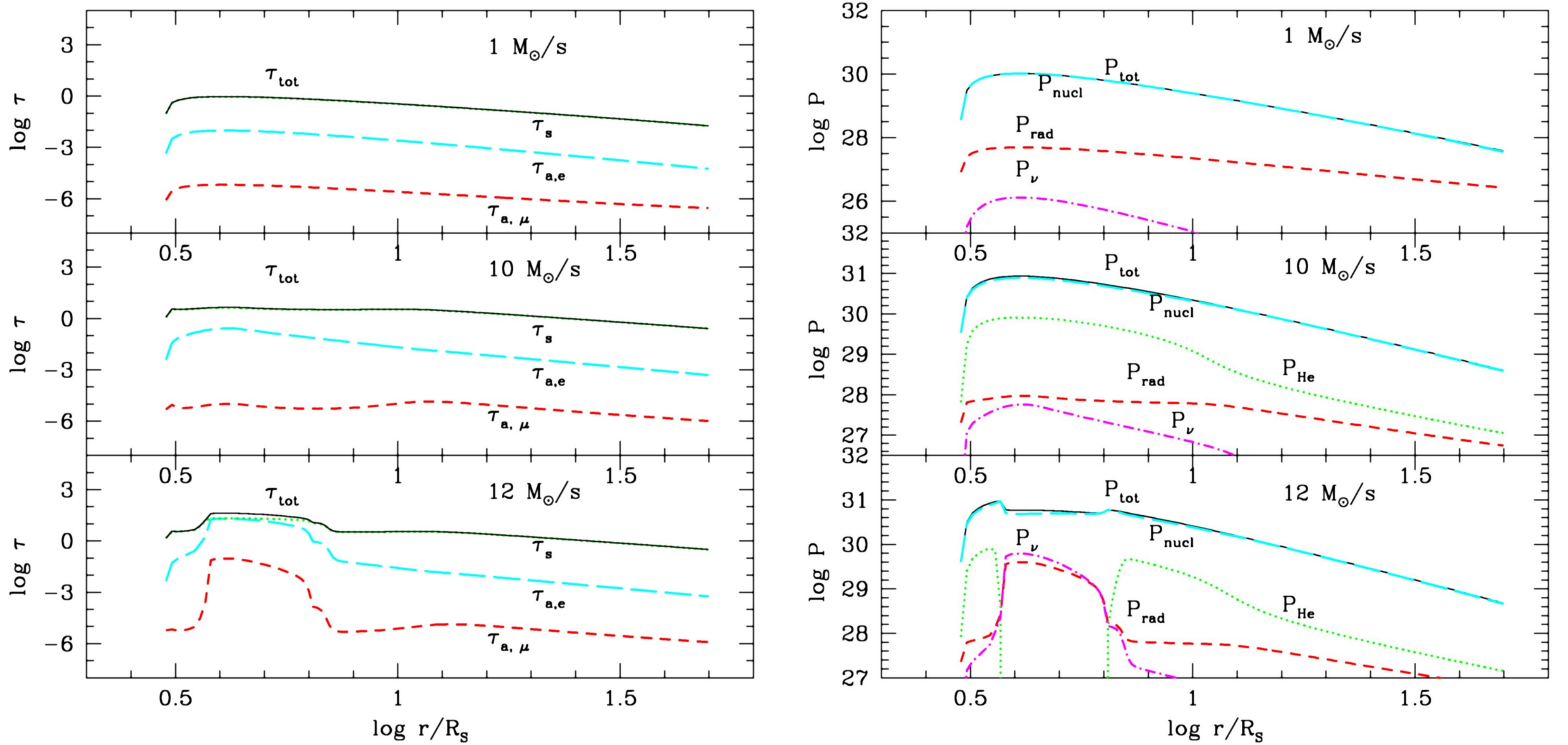

Janiuk A. Yuan Y., Perna R., Di Matteo T., 2007, ApJ, 664, 1011

BH rotation

- For rotating black hole, the inner edge of the disk moves closer to it, depending on $a = cJ/GM^2$
- We need to modify also the viscous heating, Keplerian rotation and disk height, accordingly to black hole spin a, still within a standard alpha-disk model

$$A = 1 - \frac{2GM}{c^2 r} + \left(\frac{GMa}{c^2 r}\right)^2$$

$$B = 1 - \frac{3GM}{c^2 r} + 2a\left(\frac{GM}{c^2 r}\right)^{3/2}$$

$$C = 1 - 4a\left(\frac{GM}{c^2 r}\right)^{3/2} + 3\left(\frac{GMa}{c^2 r}\right)^2$$

$$D = \frac{1}{2\sqrt{r}} \int_{r_{\rm ms}}^{r} \frac{\frac{x^2c^4}{G^2} - 6\frac{Mxc^2}{G} + 8a\sqrt{\frac{M^3xc^2}{G}} - 3a^2M^2}{\sqrt{x}\left(\frac{x^2c^4}{G^2} - 3\frac{Mxc^2}{G} + 2a\sqrt{\frac{M^3xc^2}{G}}\right)} dx$$

Novikov & Thorne (1973); Riffert & Herold (1995)

Transfer of BH rotational energy to the disk

- Open field lines:
  - Extraction of BH rotation energy through the Blandford-Znajek process
- Closed field lines:
  - On the disk surface and BH horizon the electromotive force is induced
  - Additional torque → leads to disk extra heating
  - Energy of BH rotation may be transferred to the disk

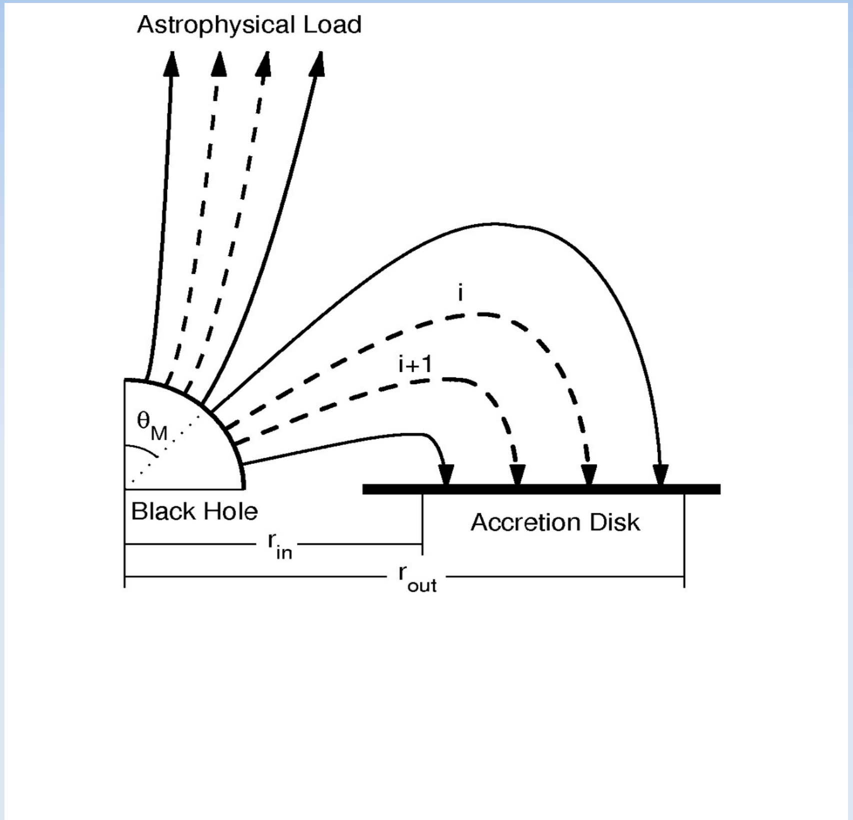

McDonald &Thorne (1982);
van Putten (1999);
Li & Paczyński (2000); Li (2000; 2002)
Wang et al (2002)

Transfer of BH rotation to the disk

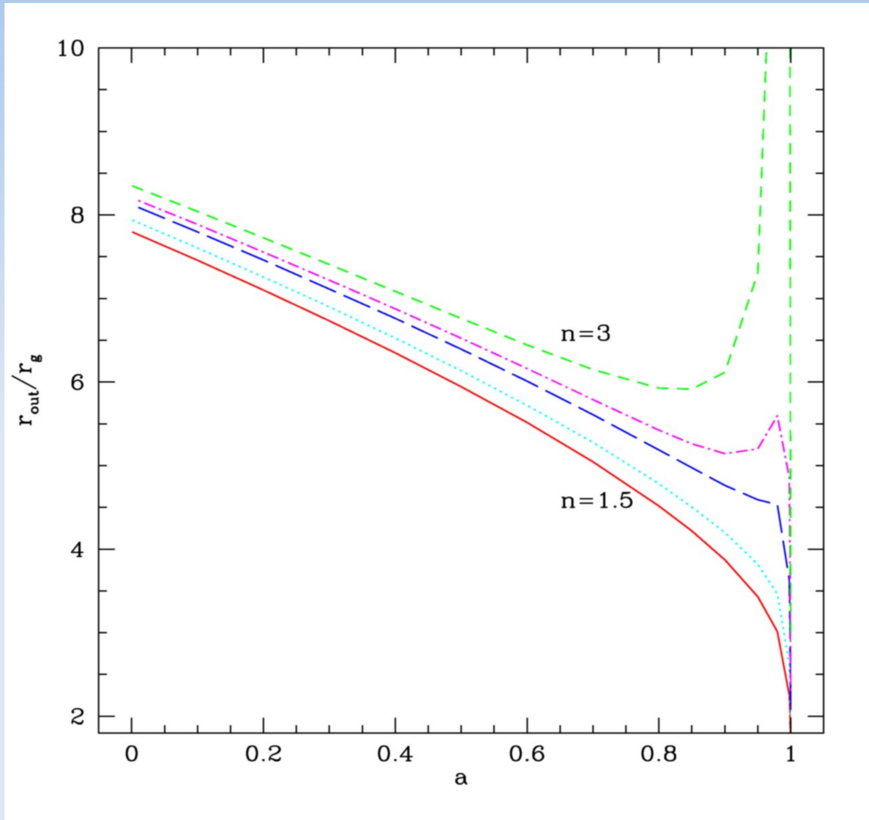

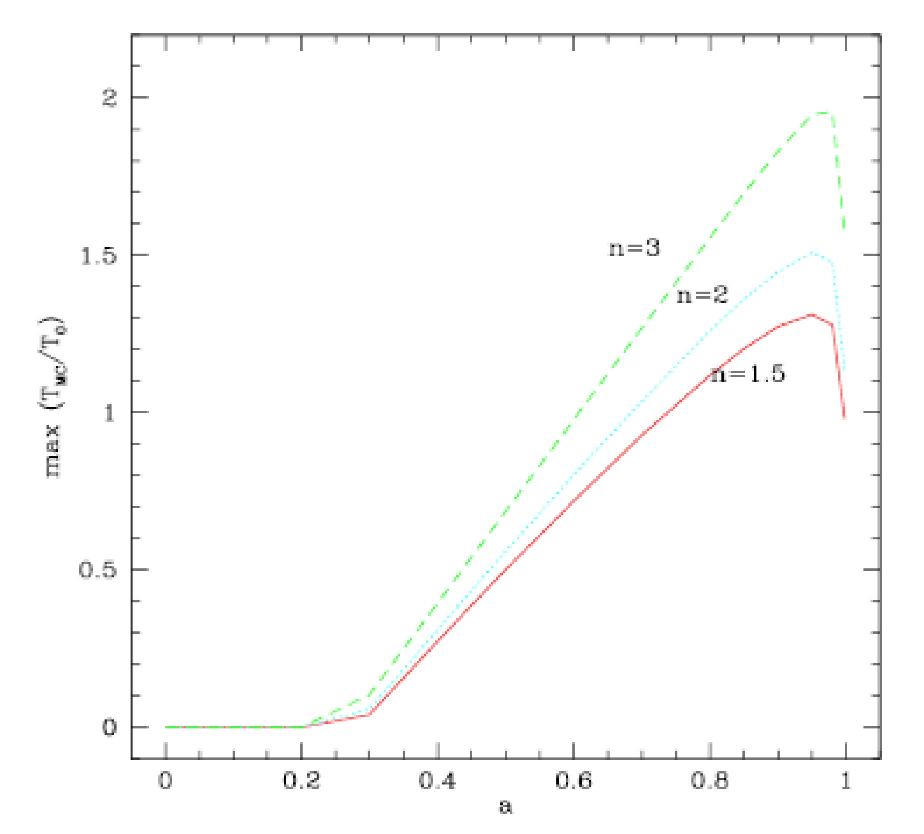

Janiuk & Yuan, 2010

Topology of B field: assumed $B_z \sim \xi^{-n}$

Torque is positive, if BH rotates faster than the differentially rotating disk, $\Omega_H > \Omega_D$

Torque normalization: equipartition $B_H^2/8\pi P_{max} = \beta_{mag} \sim \alpha$

Number densities of free particles

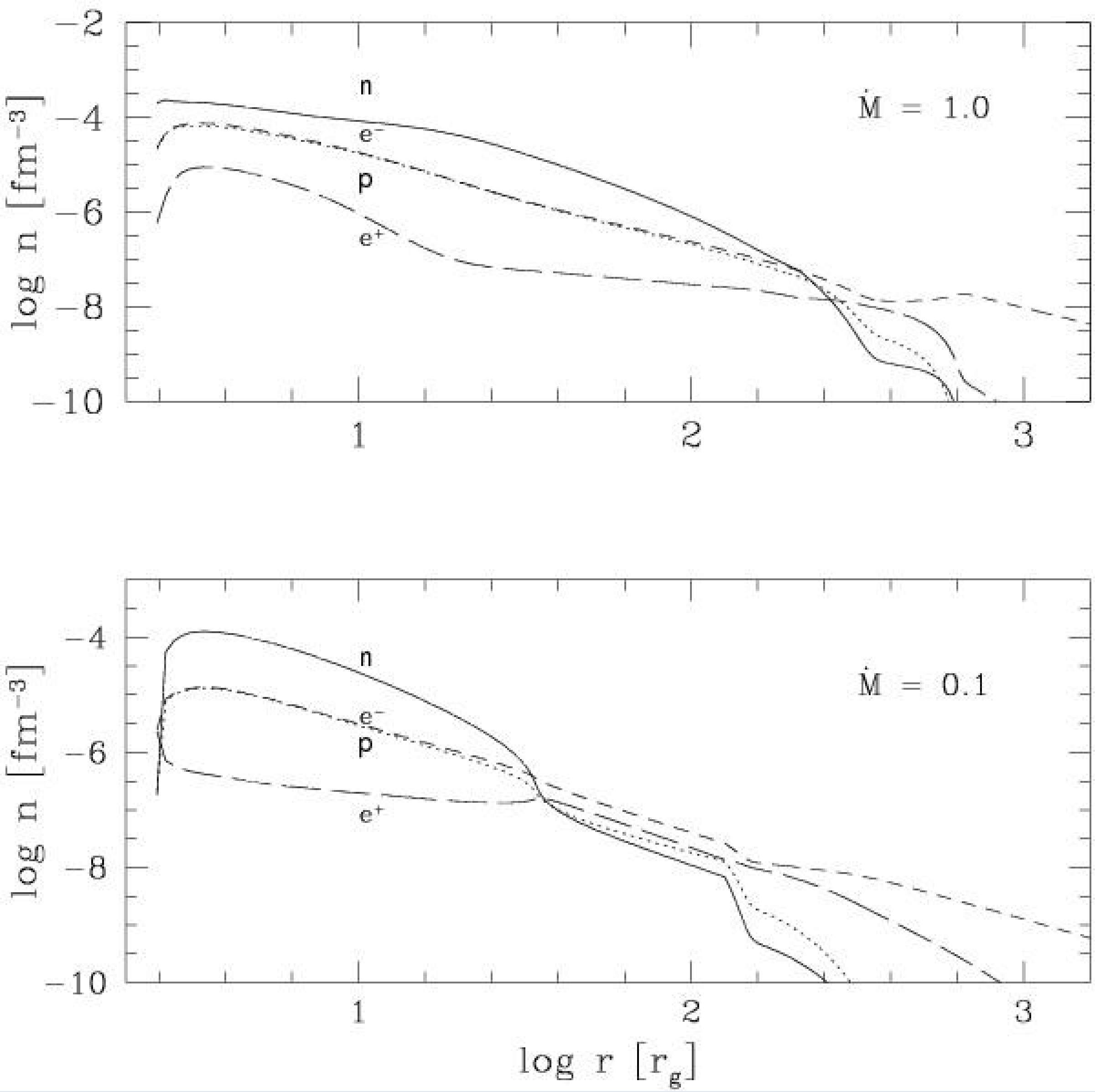

Number density of free particles as a function of distance in the accreting disk.

We show neutrons (solid line), protons (dotted line), electrons (short dashed line), and positrons (long dashed line).

The steady-state models were calculated for $\dot{M}$ = 1.0 M⊙ s^{-1} (top panel) and $\dot{M}$ = 0.1 M⊙ s-1 (bottom panel). The assumed black hole spin parameter a = 0.9.

Nucleosynthesis in the disk

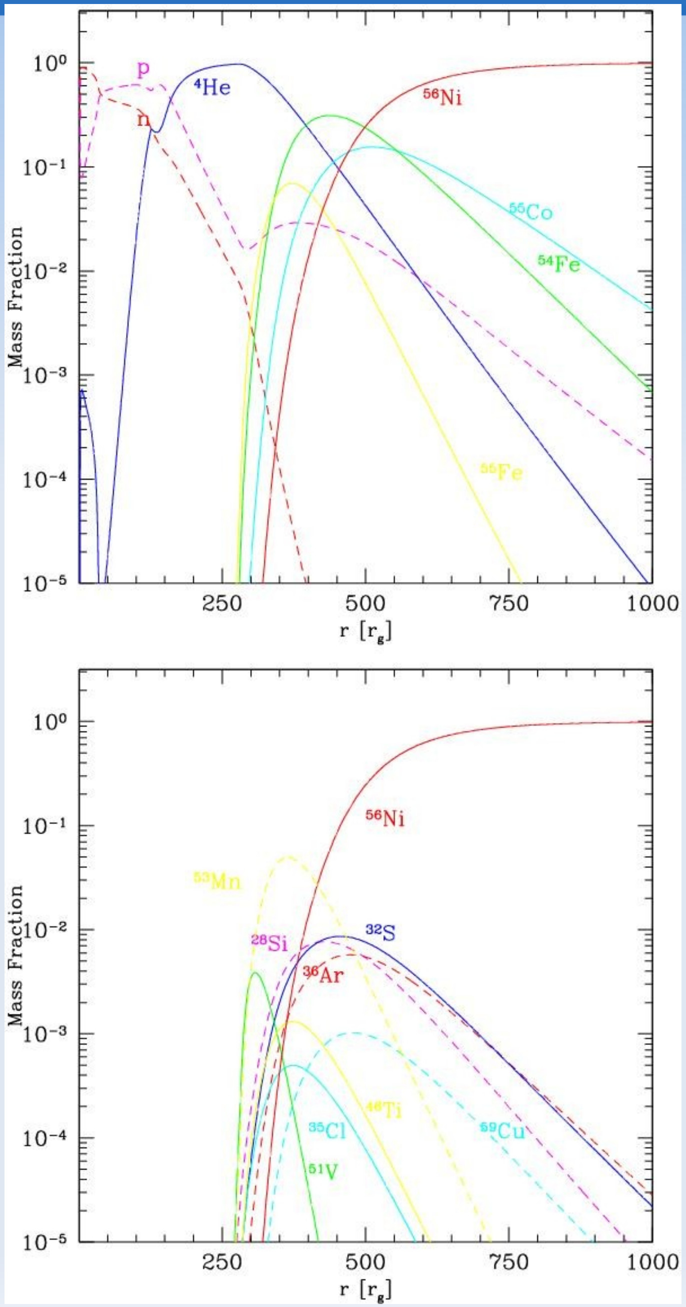

Nucleosynthesis of heavy elements in the GRB accretion disk.

The steady-state model is calculated for an accretion rate of $\dot{M} = 0.1\ M_\odot\ s^{-1}$ and a black hole spin a = 0.9.

The top panel shows the abundance distribution of free protons and neutrons (dashed lines), as well as helium, and the most abundant isotopes of nickel, iron, and cobalt.

The bottom panel shows the distribution of the most abundant isotopes of silicon, sulphur, clorium, argonium, manganium, titatnium, vanadium, and cuprum.

Janiuk A., 2014, A&A, 568, 105

1-D Model of Central engine

- We model the GRB central engine as a differentially rotating accretion disk, with extremely large accretion rates and hence at nuclear densities and temperatures
- The disk can be magnetically coupled to the spinning black hole
- Thermal instabilities due to high neutrino pressure and/or Helium photodissociacion may arise in the innermost radii of this disk
- In the magnetically coupled region extra torque is induced by the rotatig black hole and electromotive force

Summary of GRB Central engine

- The extra torque at inner radii due to MC coupling with BH seems not to stabilize the disk (Lei et al. 2009).
- The gravitational instability present at large radii.
- Such instabilities are plausible to explain the variable energy output from the engine (hence, variable Lorentz factors within the remote jets, internal shocks, GRB variability etc.)
- In the outer parts of the disk, elements heavier than Helium may be synthesized, under nuclear statistical equlibrium conditions

2D numerical simulation

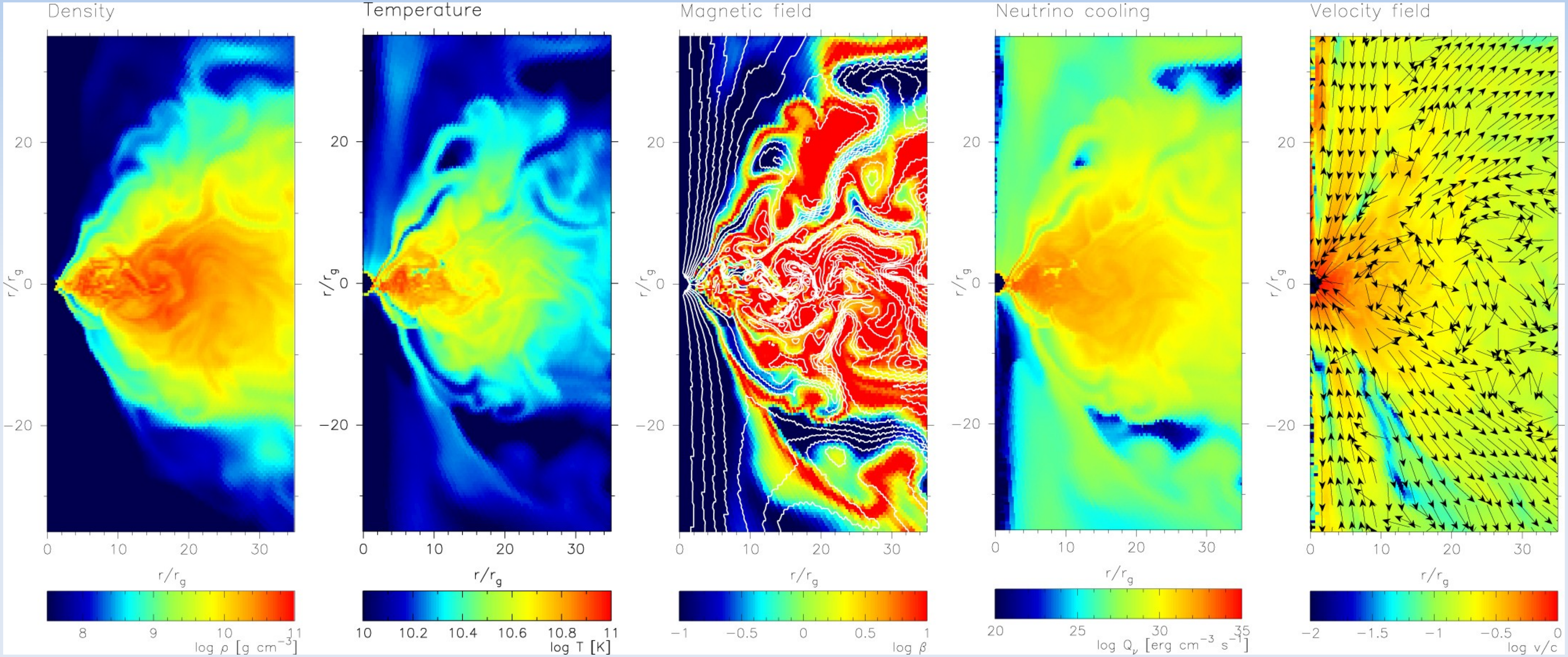

Evolved GR MHD model of accretion onto BH in the central engine, which accounts for the neutrino cooling and nuclear EOS. The maps show (i) density, (ii) temperature of the plasma, (iii) ratio of gas to magnetic pressure, with field line topology, (iv) neutrino emissivity, and (v) velocity field (from left to right). (Janiuk A., 2017, ApJ)

EOS: equation of state in numerical simulations

- Typical simulations of accretion in GR MHD were suited for modeling disks and jet ejection in Galaxy center (low densities, moderate temperatures)
- Hot and dense plasma in GRB engines requires numerical (non-linear in density and temperature) equation of state
- Technically, non-relativistic (M)HD copes with that well. GR simulations cover the engine with complex inversion schemes.
- Jet base with GR, non-GR hydro for larger scales

Neutrino vs. BZ luminosity

- Neutrinos in GRB central engine are produced in the reactions of electron and positron capture on nucleons, the electron–positron pair anihillation, nucleon bremsstrahlung, and plasmon decay.
- The total neutrino luminosity of the engine may exceed the luminosity computed for the Blandford-Znajek process

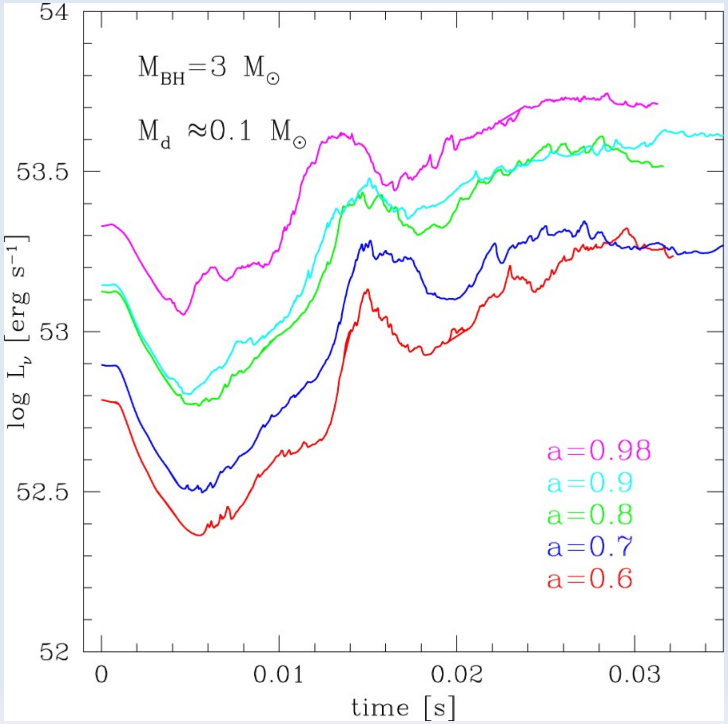

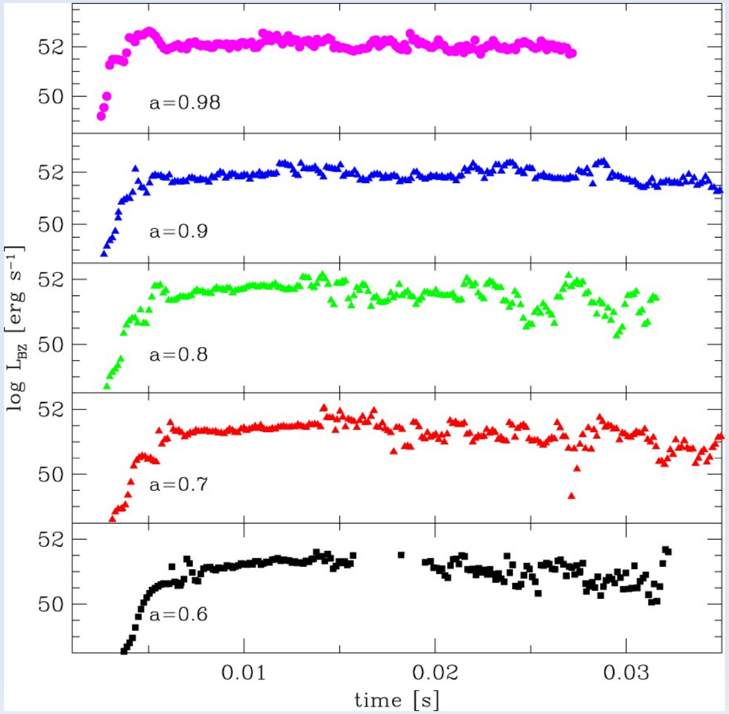

Tracer particles technique

- Tracers are passive moving particles which store information about the gas properties.
- At initail time of simulation we pick all the particles that are embedded in the densest parts of the flow
- Their coordinates, velocities, and other quantities are recorded in time, until they leave the computational domain

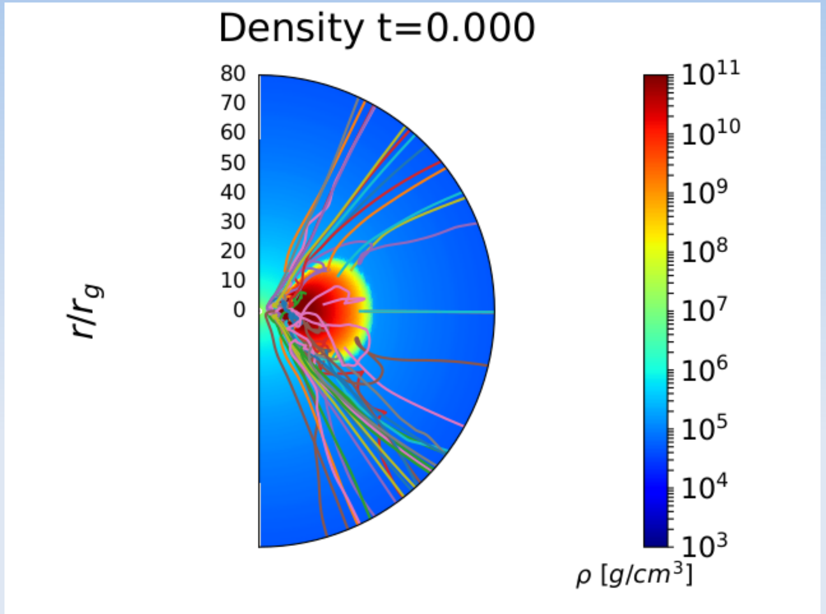

Matter is neutronized,

$$Y_e = n_p/(n_p + n_n) < 0.5.$$

Electron fraction

- Tracer particles store information about thermodynamics and chemical composition of outflows.
- Neutronised material is unbound.

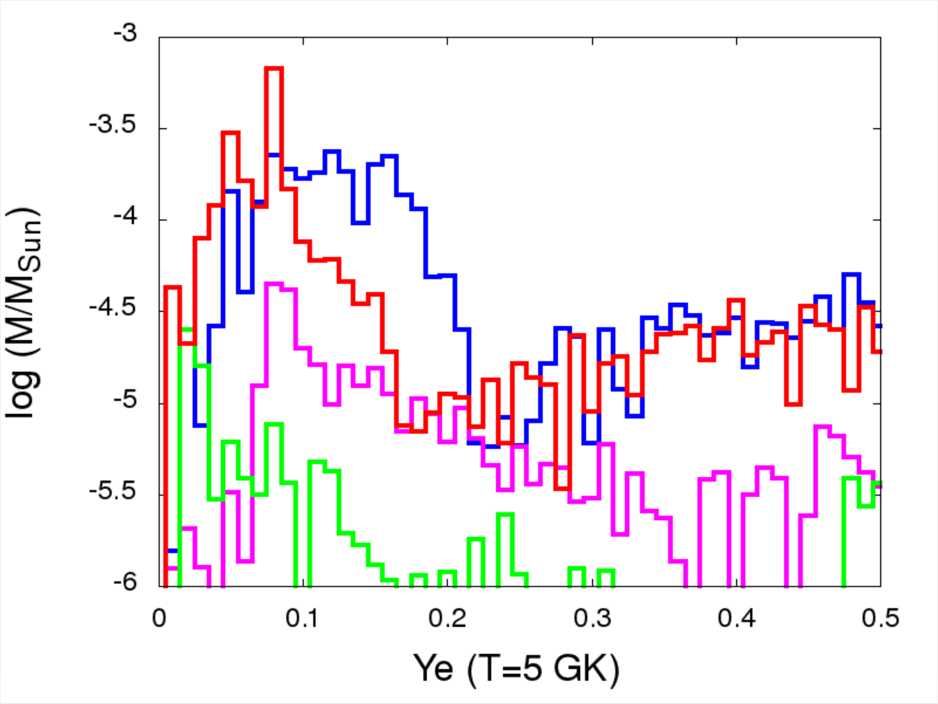

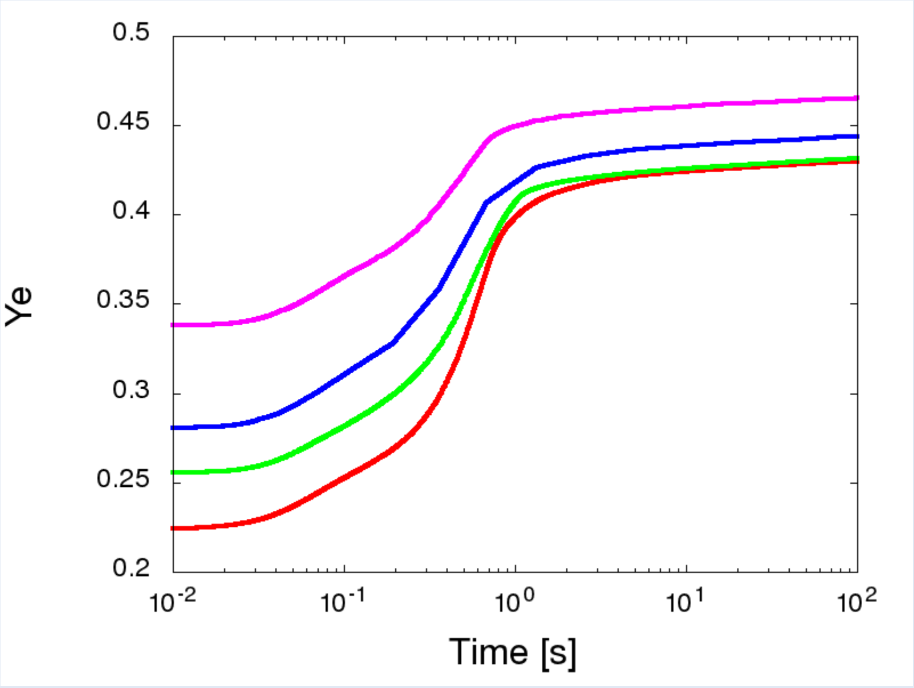

Heavy element synthesis

- Nuclear reaction networks calculate synthesis of heavy ions, over Iron-peak, via rapid neutron capture: r-process.
- This process occurs in the disk wind.
- Most of the synthesized isotopes are unstable and they decay rapidly, producing radiation.

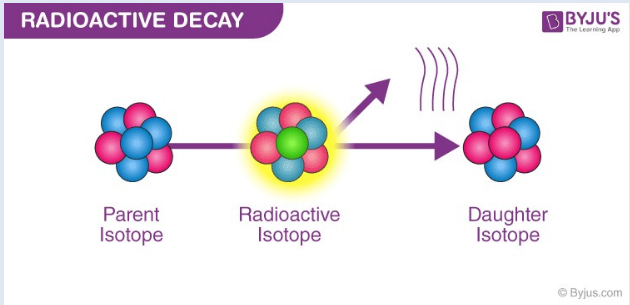

- The stable isotopes may be formed as well and they remain in the interstellar medium

r-process nucleosynthesis

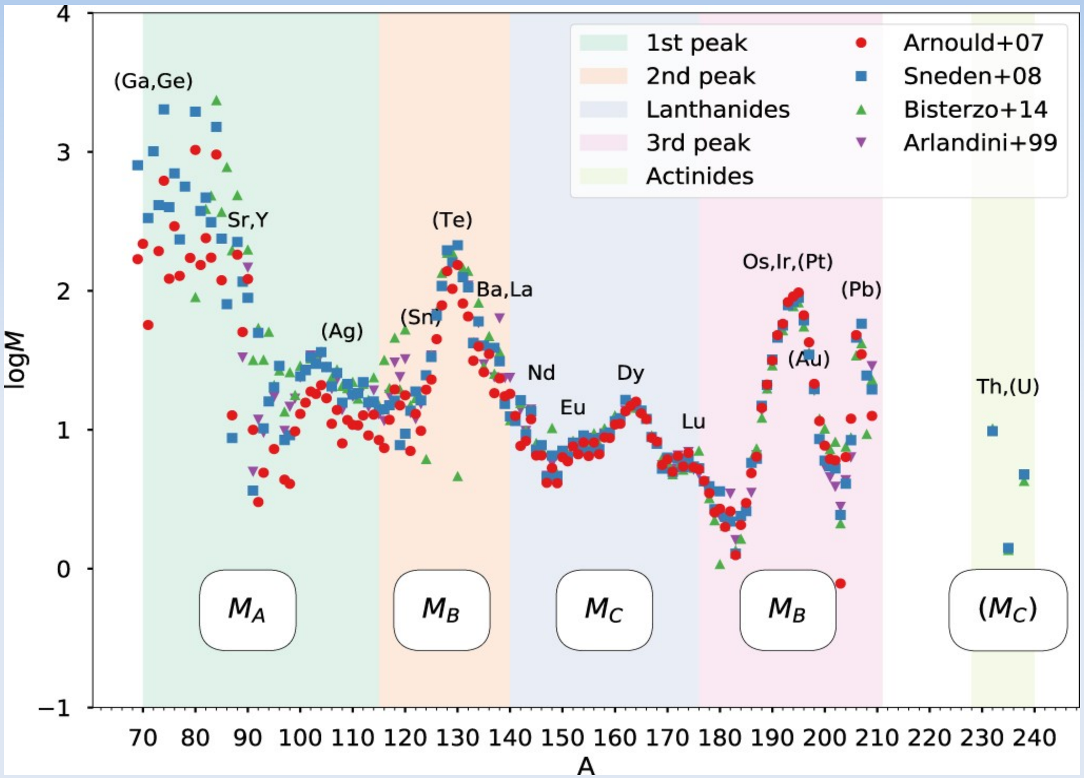

Ji et al. 2019

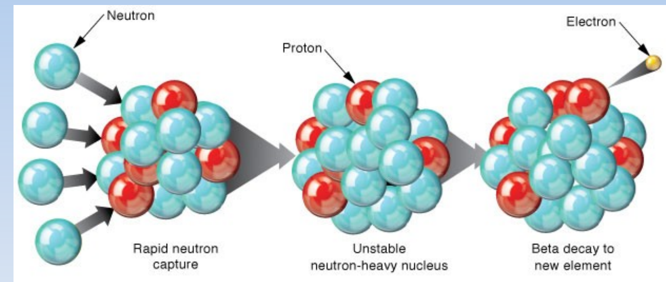

$Y_e > 0.25$: 1st peak

$Y_e = 0.15$-0.25: 2nd peak, Lanthanides

$Y_e < 0.15$: 3rd peak, Actinides

Nuclear reaction network calculations

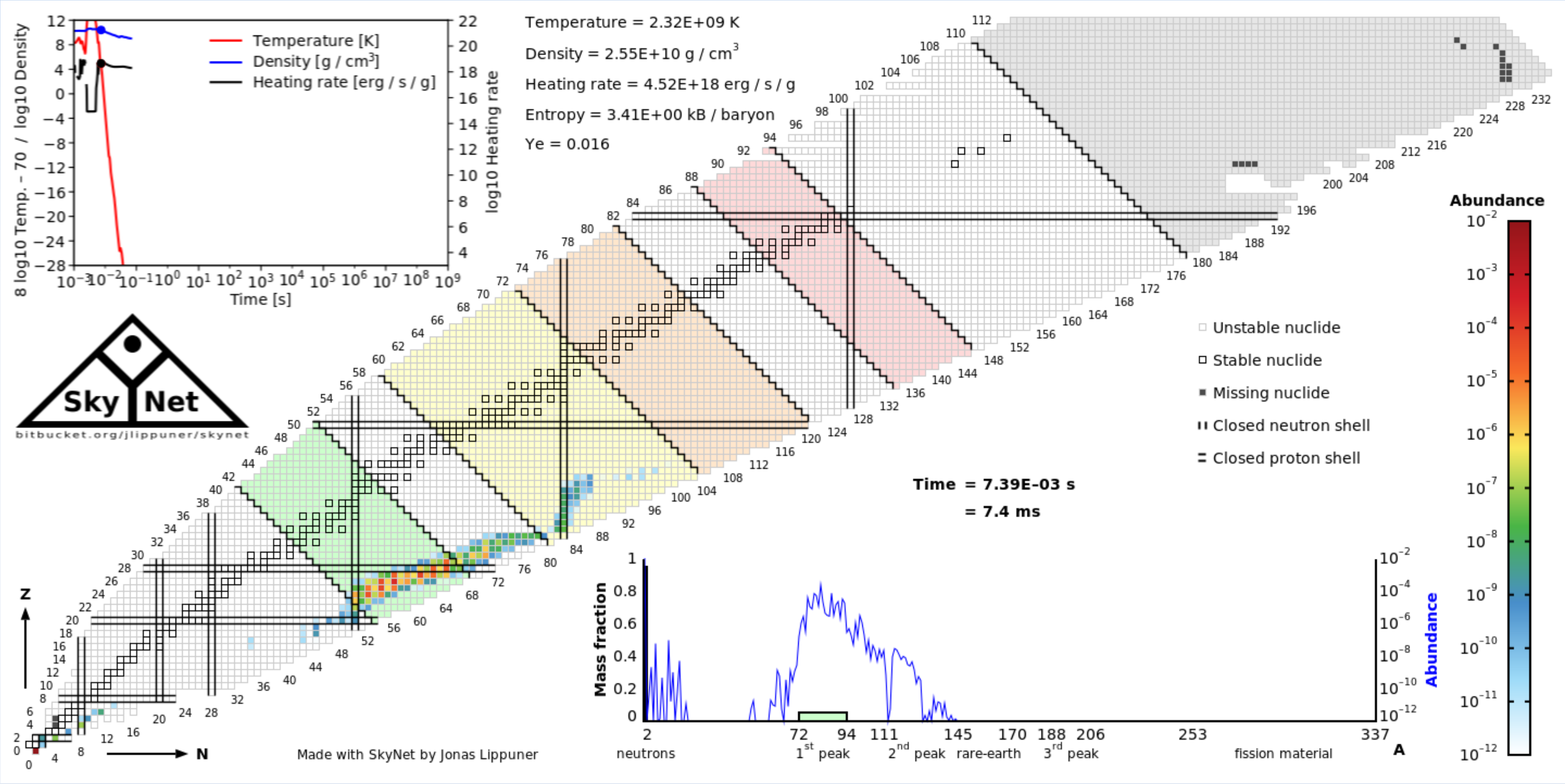

Code **SkyNet**, provides a nuclear reaction network; Lippuner & Roberts (2017).

Chemical enrichment of the ISM

- Abundance pattern of isotopes created via r-process nucleosynthesis on the GRB engine outflow traccers (grey lines)
- Average pattern (red line) is compared with Solar System data (blue points)

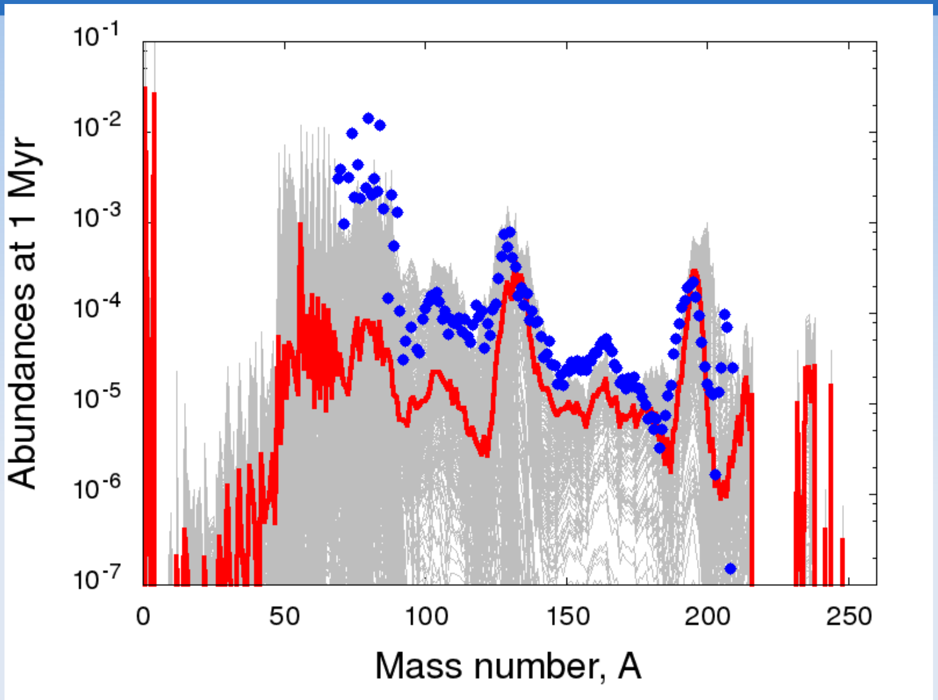

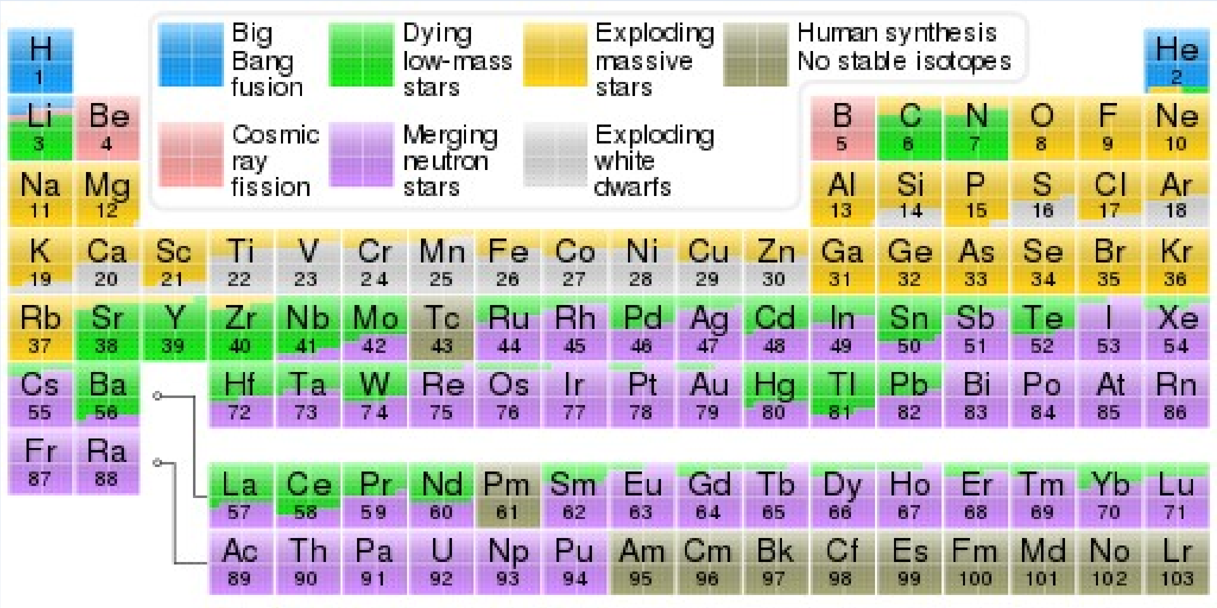

Kilonovae

- NS-NS merger ejects material rich in heavy radioactive isotopes.
- Their decay can power an electromagnetic signal called a kilonova (e.g. Li & Paczynski 1998; Tanvir et al. 2013, Berger 2016)
- Dynamical ejecta from compact binary mergers, $M_{ej} \sim 0.01\ M_{Sun}$, can emit about 10^{40}-10^{41} erg/s in a timescale of 1 week
- Subsequent accretion can provide bluer emission, if it is not absorbed by precedent ejecta (Tanaka, 2016, Berger 2016, Siegel & Metzger 2017)

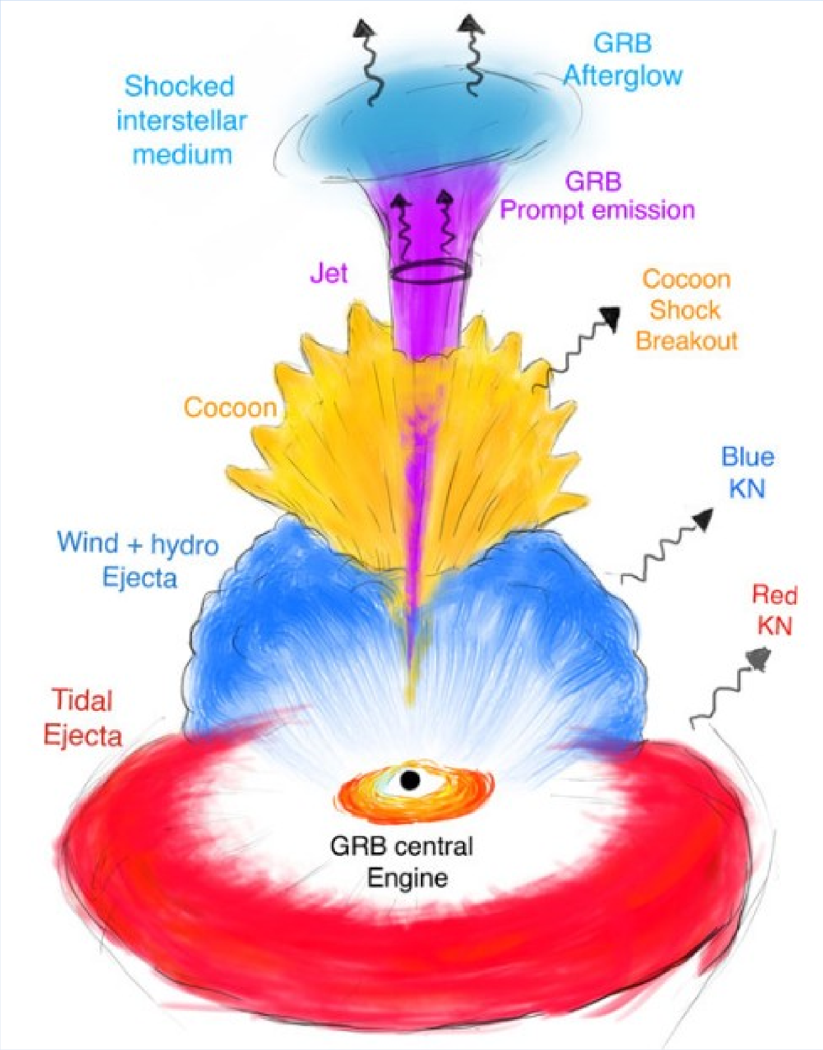

Kilonova observed in associacion with GW-GRB 170817

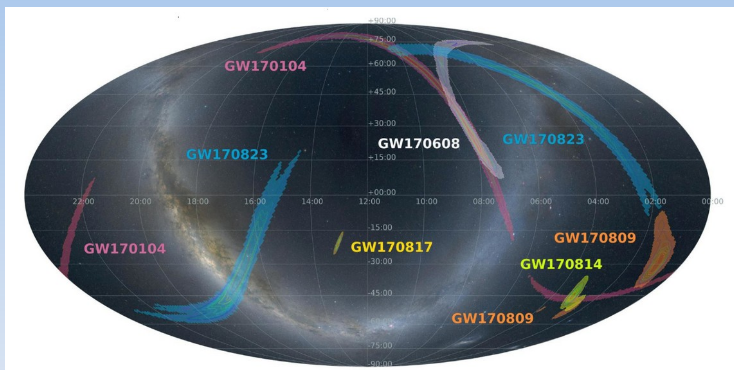

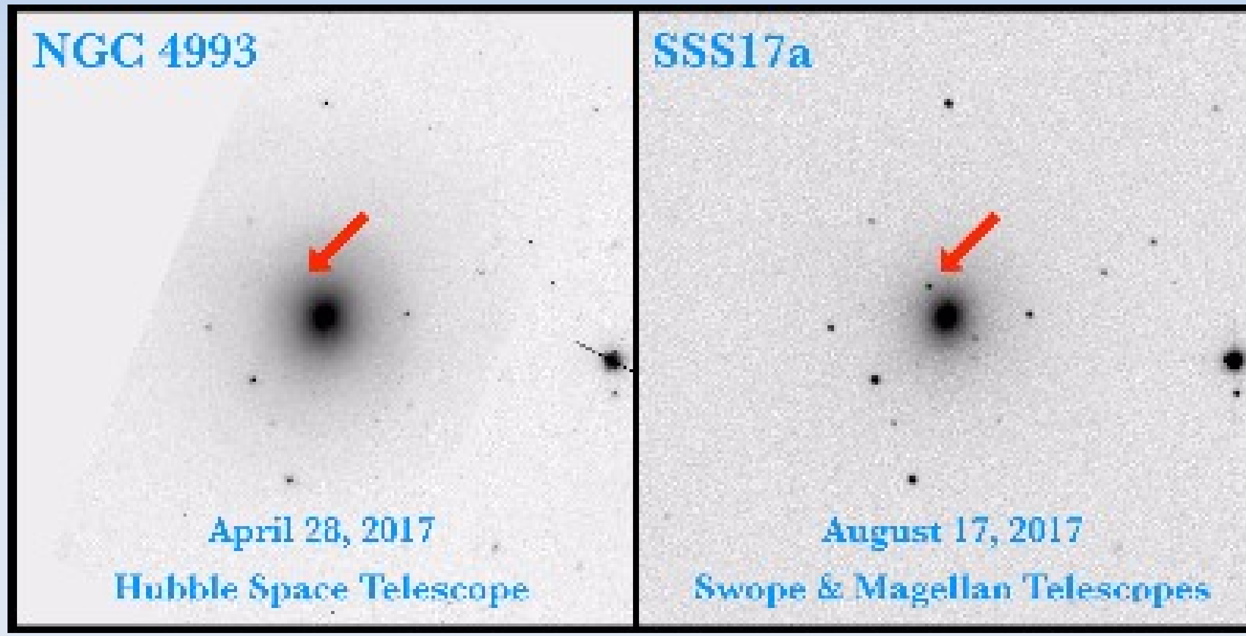

Predictions of kilonova model were verified observationally!

Rapidly fading electromagnetic transient in the galaxy NGC4993, was spatially coincident with GW170817 and the weak short gamma-ray burst (e.g., Smartt et al. 2017)

Blue and red kilonova lightcurves

- Blue and the red light from a kilonova, originate from media with different opacities due to Lanthanide contributions
- Components give separate fits to observational data for the transient SSS17a, associated with GW170817 (Kilpatrick et al. 2017).

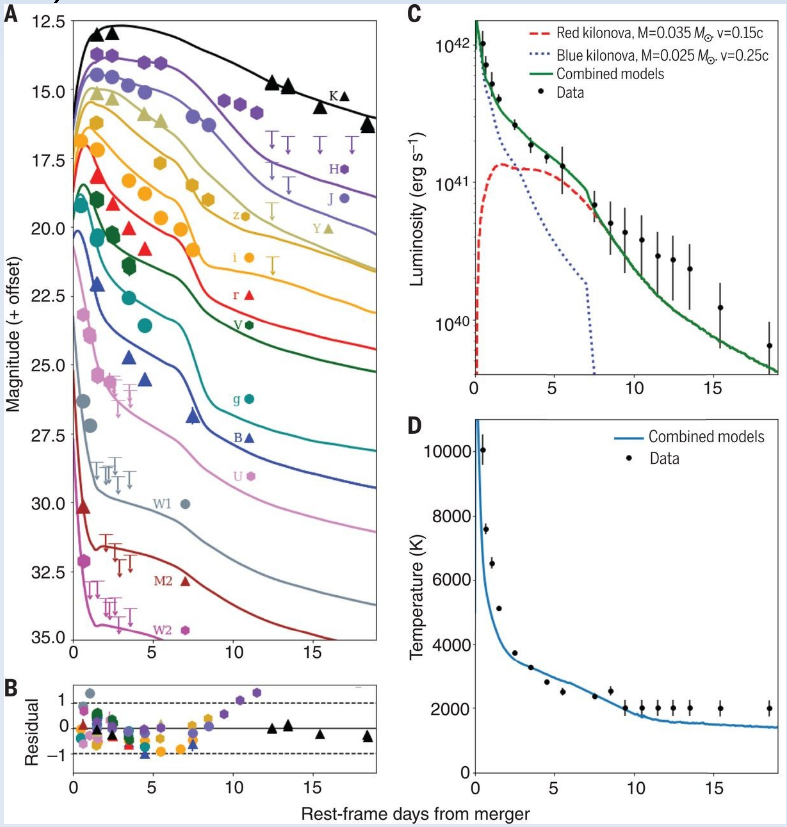

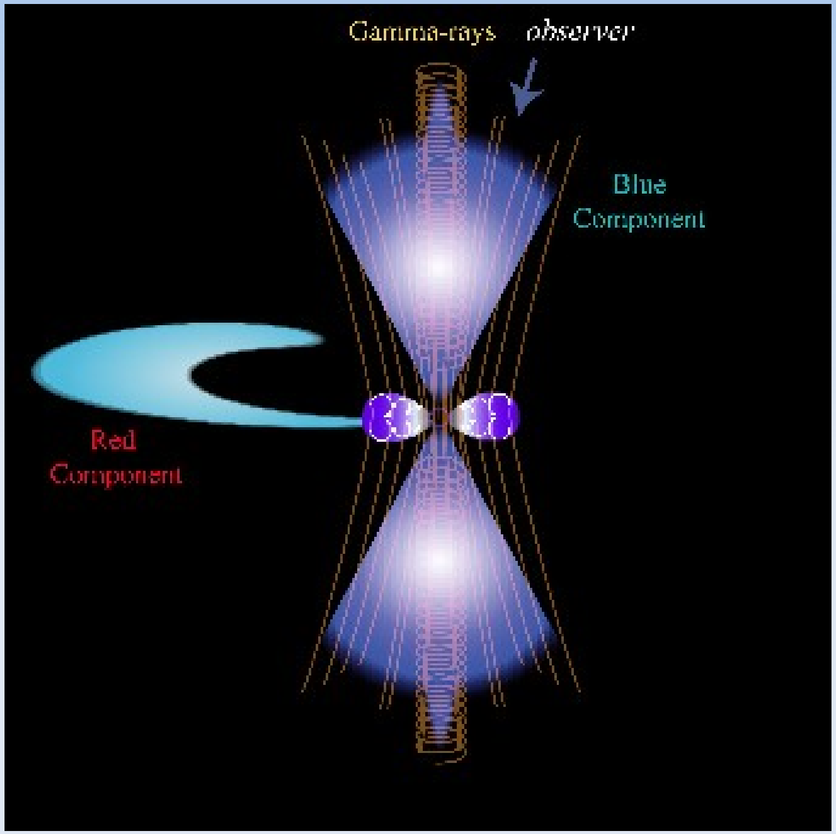

Schematic idea of the GW170817 system in the post-merger phase (Murguia-Berthier et al. 2017).

Next week

- Neutron stars, structure
- NS models, maximal mass, equations of state.

Further reading suggested:

1) M.G. Bernardini, ”Gamma-ray bursts and magnetars: Observational signatures and predictions”, Journal of High Energy Astrophysics, 7, 64 (2015)